Supporting Information

for

Single Molecular Multi-analyte (Al^{3+}, Cr^{3+} and Fe^{3+}) Fluorescent Probe in Aqueous and Its Biological Applications

Junfeng Wang,[a] Yingbo Li,[c] Nikul G. Patel,[d] Ge Zhang,[d] Demin Zhou[c] & Yi Pang[a,b]*

[a]Department of Chemistry & [b]Maurice Morton Institute of Polymer Science, [d]Department of Biomedical Engineering, The University of Akron, Akron, Ohio 44325 U.S.A; E-mail: yp5@uakron.edu

[c]State Key Laboratory of Natural and Biomimetic Drugs, School of Pharmaceutical Sciences, Peking University, Beijing 100191, China

Synthesis of intermediate A

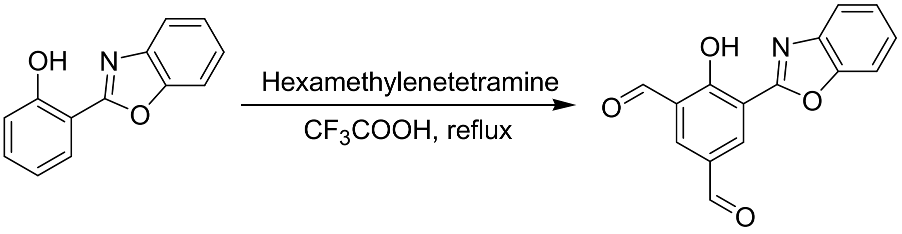

A

Intermediate **A** was synthesized by a modified procedure. 2-(2’-hydroxyphenyl)benzoxazole (570 mg), purchased from Aldrich Chemical, was dissolved in CF_3COOH (10 mL), then hexamethylenetetramine (1057 mg) was added in one portion. The resulting mixture was refluxed and monitored by TLC until the starting material disappeared (2 days). Then 10 mL water was added slowly and the resulting mixture was refluxed for another 10 mins until yellow solid precipitated out. Product A was achieved by simple filtration as pure product in quantitative yield as yellow solid, which could be further purified by a short pad of silica as white solid, which is identical to our previous data (*Org. Lett.,* 2011**, 13**, 1262). ^{1}H NMR (300 MHz, $CDCl_3$): 13.04 (1H, s), 10.64 (1H, s), 10.02 (1H, s), 8.83 (1H, s), 8.49 (1H, s), 7.80 (1H, d, *J* = 6.3 Hz), 7.69 (1H, d, *J* = 6.0 Hz), (1H, d, *J* = 8.4 Hz), 7.50-7.44 (2H, m).

Synthesis of dye 1

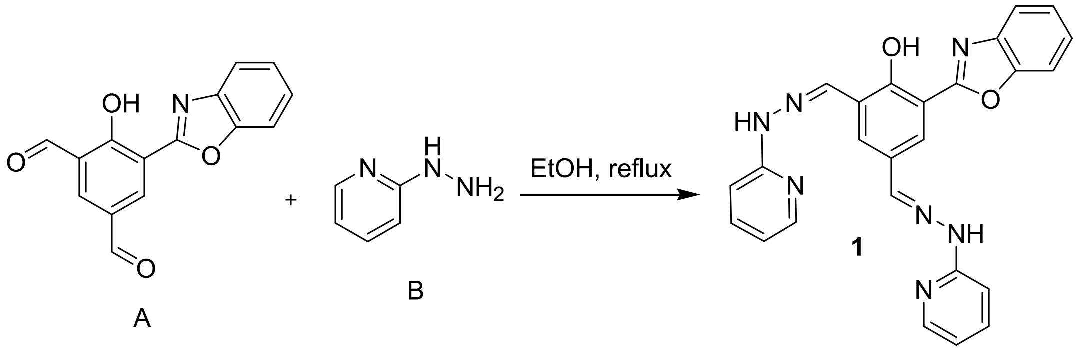

Intermediates **A** (80.0 mg) and **B** (70.0 mg) were dissolved in EtOH, then the reaction mixture was refluxed for 2 hours. Dye **1** precipitated out as yellow solid and was purified by simple filtration in >90% yield. ^{1}H NMR (300 MHz, DMSO-*d*$_6$): 12.08 (1H, s), 11.10 (1H, s), 10.85 (1H, s), 8.46 (1H, s), 8.24 (2H, d, *J* = 11.7 Hz), 8.14-8.10 (3H, m), 7.88 (2H, tri, *J* = 6.0 Hz), 7.68 (2H, tri, *J* = 7.5 Hz), 7.52-7.44 (2H, m), 7.24 (2H, tri, *J* = 7.5 Hz), 6.79 (1H, d, *J* = 7.5 Hz), 6.76 (1H, d, *J* = 7.5 Hz); ^{13}C NMR (75 MHz, DMSO-*d*$_6$): 162.3, 157.5, 157.1, 156.0, 149.4, 148.3, 148.3, 139.8, 138.5, 138.4, 138.3, 134.6, 128.0, 127.2, 126.6, 125.9, 124.7, 124.0, 119.8, 115.8, 115.4, 112.1, 111.7, 107.0, 106.7. HRMS (m/z): calcd for $C_{25}H_{20}N_7O_2$, $[M+H^+]^+$, 450.1678, found, 450.1693; HRMS (m/z): calcd for $C_{25}H_{19}N_7O_2Na$, $[M+Na^+]^+$, 472.1498, found, 472.1489.

Synthesis of dye 4

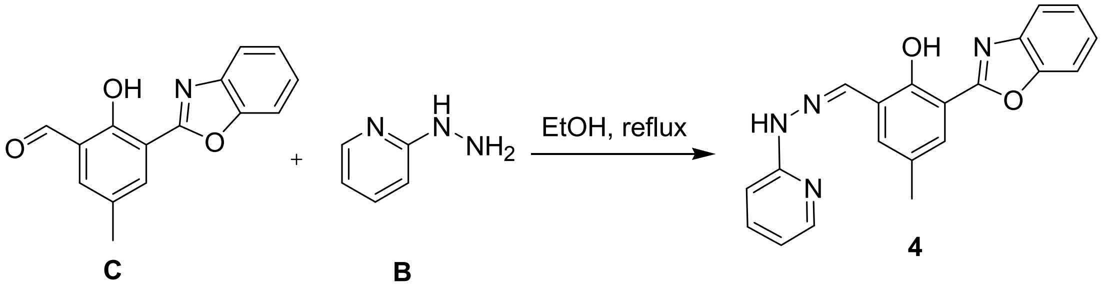

Intermediates **C**^{1} (50.0 mg) and **B** (27.0 mg) were dissolved in EtOH. The reaction mixture was refluxed for 2 hours. Dye **4** precipitated out as yellow solid and was purified by simple filtration in >90% yield. ^{1}H NMR (300 MHz, DMSO-*d*$_6$): 11.66 (1H, s), 11.00 (1H, s), 8.43 (1H, s), 8.11 (1H, d, *J* = 3.9 Hz), 7.87-7.82 (3H, m), 7.64 (1H, tri, *J* = 6.9 Hz), 7.51-7.44 (2H, m), 7.24 (1H, d, *J* = 8.4 Hz), 6.77 (1H, tri, *J* = 6.0 Hz), 2.38 (3H, s);

^{13}C NMR (75 MHz, DMSO-d_6): 162.6, 157.3, 153.9, 149.2, 148.3, 139.8, 138.3, 134.6, 130.2, 129.3, 127.9, 126.4, 125.8, 123.5, 119.6, 115.5, 111.5, 111.1, 106.9, 20.5. HRMS (m/z): calcd for $C_{25}H_{20}N_7O_2$, [M+H$^+$]$^+$, 450.1678, found, 450.1693; TOF-MS-ES$^+$ (m/z): calcd for $C_{20}H_{17}N_4O_2$, [M+H]$^+$, 345.1352, found, 345.1729; calcd for $C_{20}H_{16}N_4O_2Na$, [M+Na]$^+$, 367.1171, found, 367.1540; calcd for $C_{20}H_{16}N_4O_2K$, [M+K]$^+$, 383.0910, found, 383.1324.

Synthesis of intermediate D

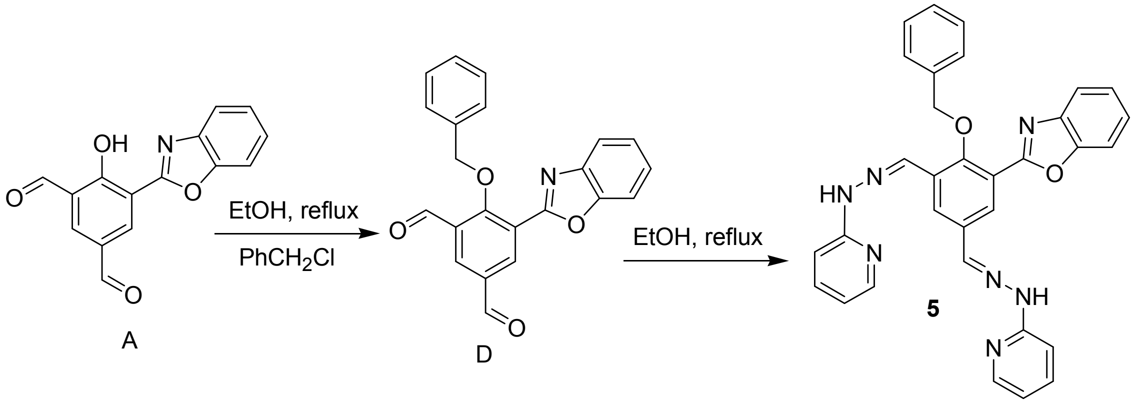

The intermediate **A** (267 mg) and benzyl chloride (250 mg) were dissolved in EtOH. The reaction mixture was refluxed overnight. Intermediate C was purified by flash column chromatography on silica gel by eluting with EtOAc/Hexanes (1:7) to afford the desired product as a white solid (203 mg, 57%) . ^1H NMR (300 MHz, DMSO-d_6): 10.25 (1H, s), 10.11 (1H, s), 8.98 (1H, d, $J = 2.1$ Hz), 8.48 (1H, d, $J = 1.8$ Hz), 7.89-7.86 (1H, m), 7.65-7.62 (1H, m), 7.47-7.44 (2H, m), 7.37 (5H, m), 5.26 (2H, s); ^{13}C NMR (75 MHz, DMSO-d_6): 189.4, 188.1, 164.2, 158.6, 150.5, 141.7, 136.8, 134.8, 132.6, 132.6, 132.0, 129.2, 129.1, 128.8, 128.5, 126.2, 125.1, 123.5, 120.7, 110.8, 79.7.

Synthesis of 5

The intermediate **C** (157 mg) and 2-hydrazinylpyridine (150 mg) were dissolved in EtOH. The reaction mixture was refluxed for 2 hours. Dye **5** precipitated out as yellow solid and was purified by simple filtration in >90% yield. ^1H NMR (300 MHz, DMSO-d_6): 11.24 (1H, s), 10.99 (1H, s), 8.47 (1H, s), 8.39 (1H, d, $J = 2.1$ Hz), 8.35 (1H, d, $J = 2.1$ Hz), 8.16 (1H, s), 8.16-8.13 (2H, m), 7.88-7.84 (1H, m), 7.74-7.67 (3H, m), 7.61 (2H, d, $J =$

7.5 Hz), 7.49-7.42 (2H, m), 7.38 (2H, d, *J* = 7.2 Hz), 7.34 (1H, d, *J* = 4.2 Hz), 7.28 (2H, tri, *J* = 8.1 Hz), 6.82-6.77 (2H, m), 5.00 (2H, s); ^{13}C NMR (75 MHz, DMSO-d_6): 160.7, 157.4, 155.2, 150.7, 148.3, 141.7, 138.5, 137.8, 136.8, 133.4, 132.7, 131.7, 129.4, 128.7, 128.7, 127.6, 126.4, 126.2, 125.4, 122.5, 120.4, 115.8, 115.7, 111.4, 107.0, 106.8, 77.7.

1. W. Chen, Y. Xing, and Y. Pang, *Org. Lett.* **2011,** *13*, 1262-1265.

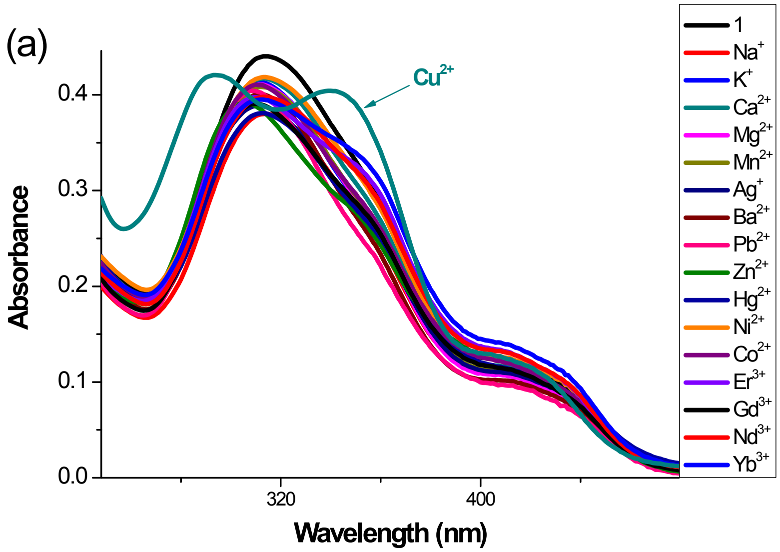

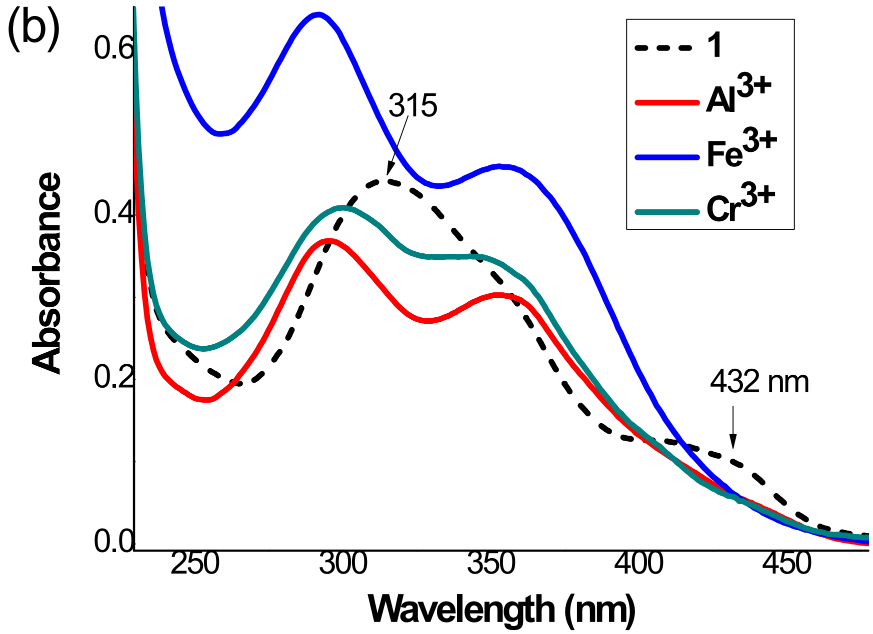

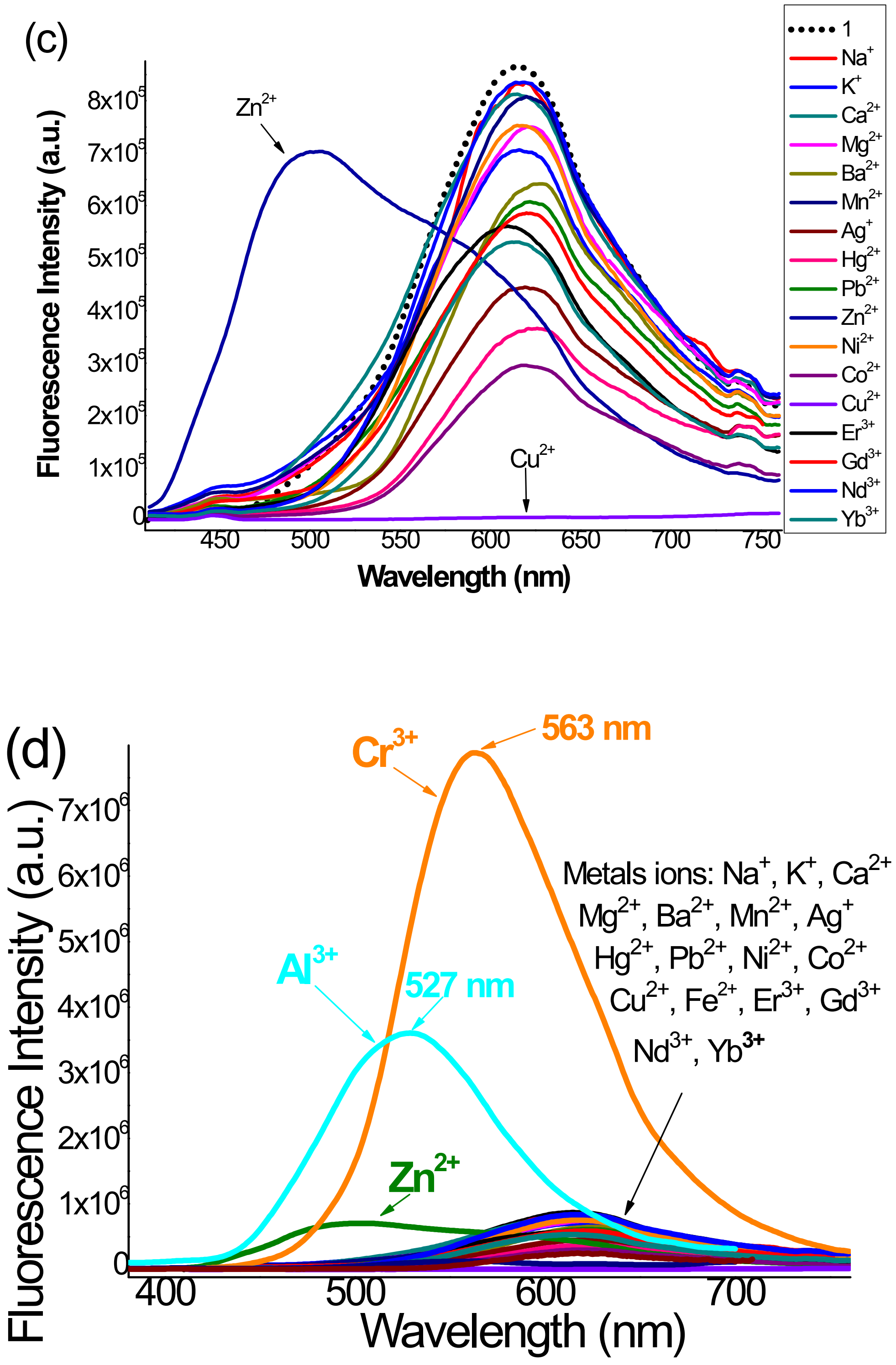

Fig. S1. UV-vis (a,b) and fluorescence spectra (c,d) of **1** upon addition of 10 equiv. of metal ions in aqueous: (H_2O:EtOH = 8:2).

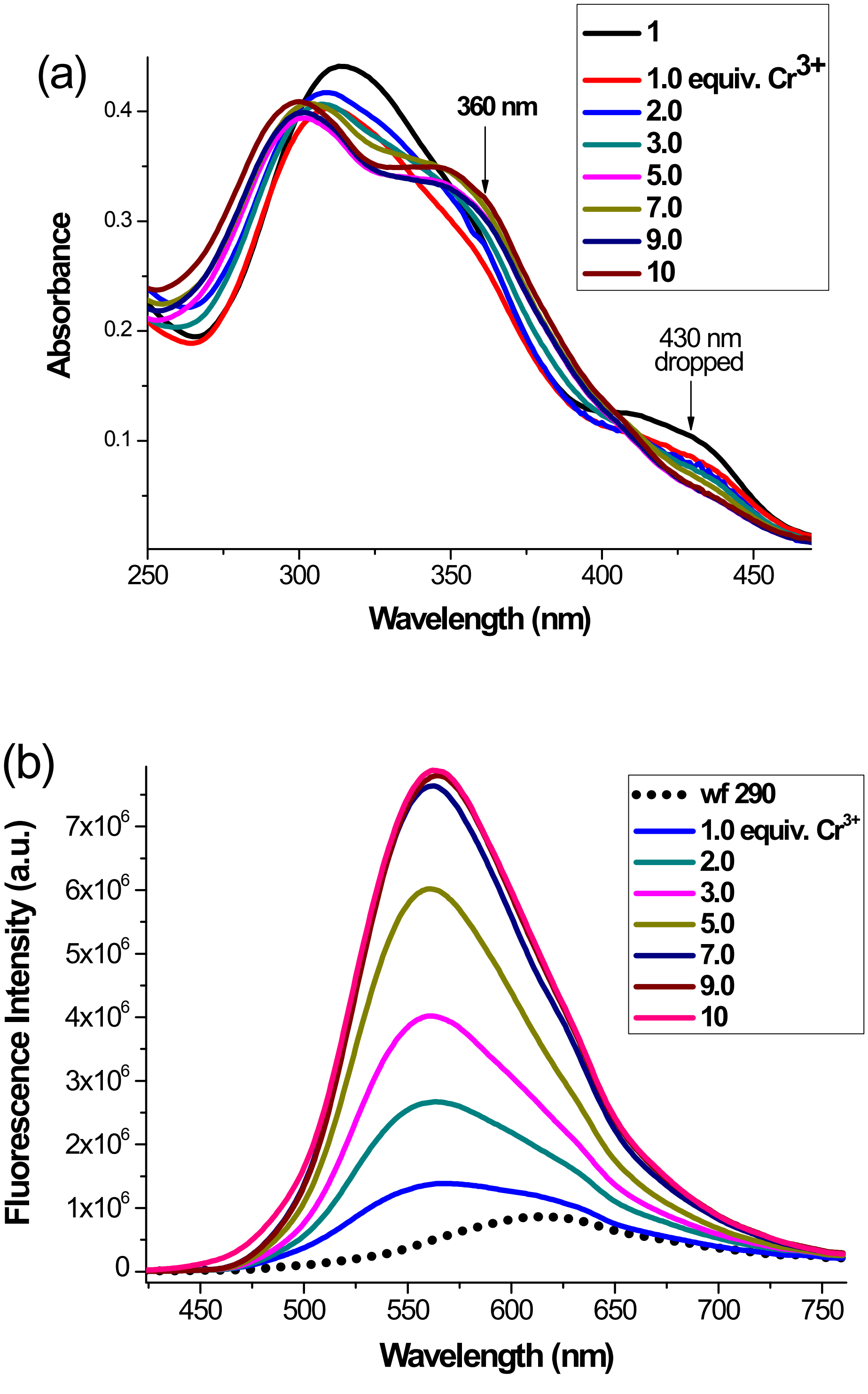

Fig. S2 UV-vis (a) and fluorescence (b) titration of **1** by addition of different equiv. of Cr^{3+} in H_2O:EtOH = 8:2.

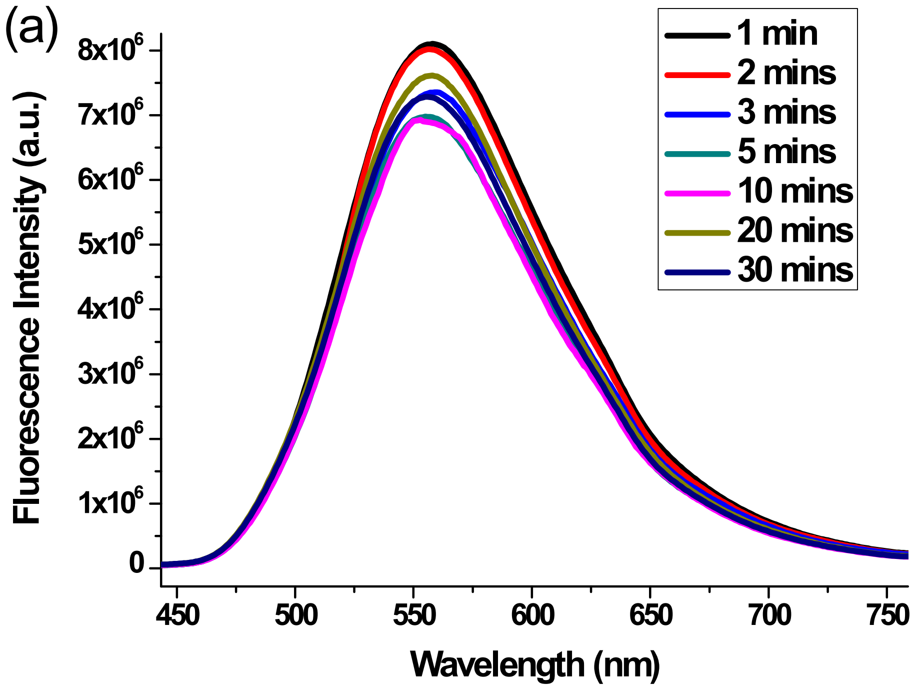

Fig. S3 Fluorescence change of **1** upon addition of 10 equiv. of Cr^{3+} in aqueous over time: (H_2O:EtOH = 8:2).

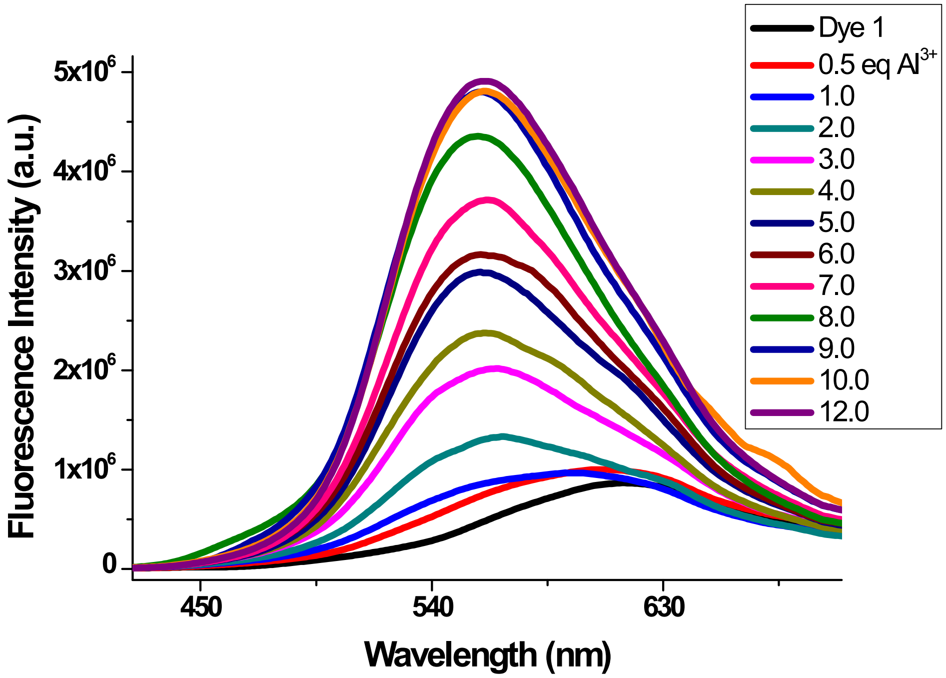

Fig. S4 Fluorescence intensity of **1** upon addition of different equivalent of Al^{3+} in H_2O:EtOH = 8:2 within 1 minute.

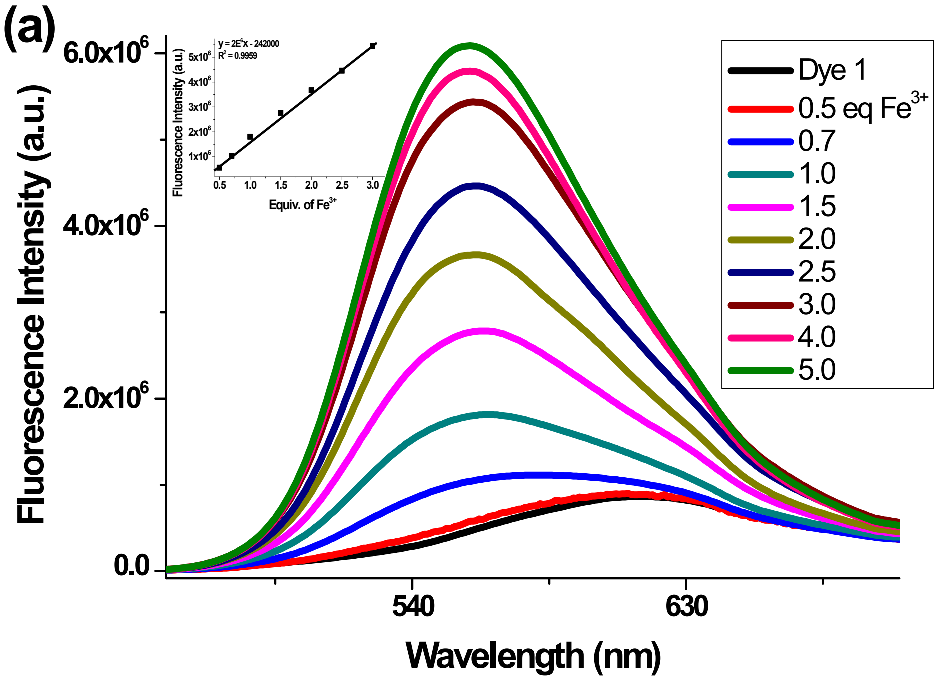

Fig. S5a Fluorescence intensity of **1** (10 μM) upon addition of different equiv. of Fe^{3+} in H_2O:EtOH = 8:2 within 1 minute.

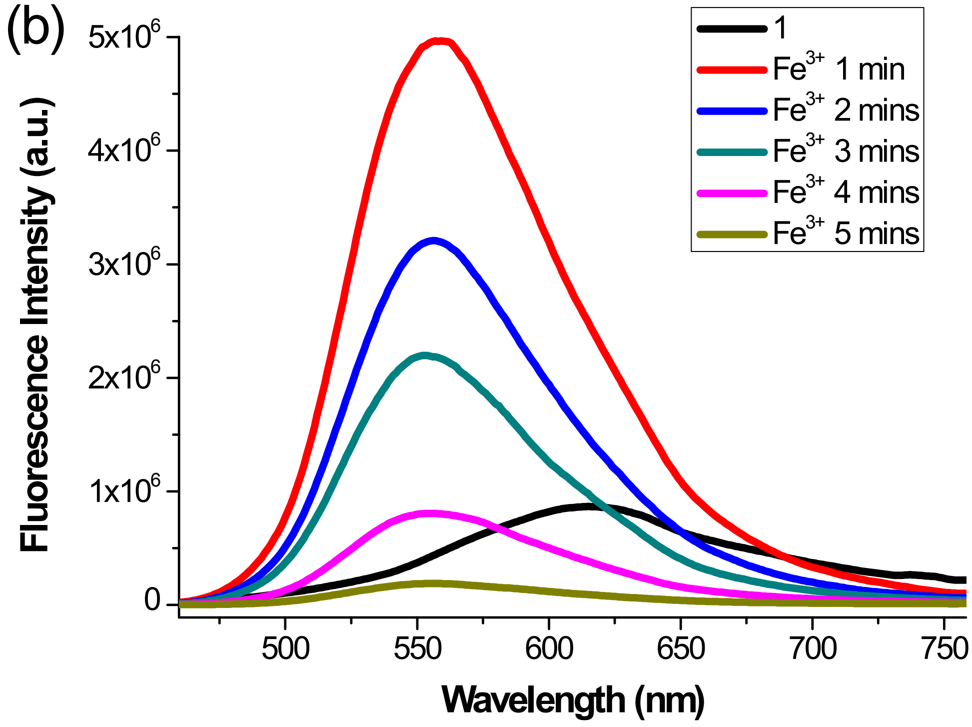

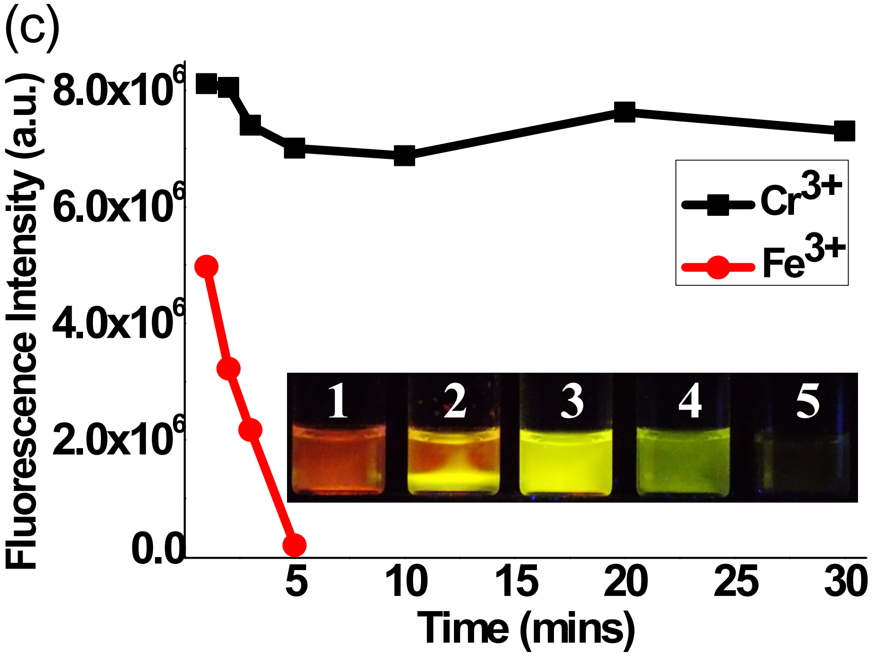

Fig. S5b Fluorescence change of **1** (10 μM) upon addition of 10 equiv. of Fe^{3+} in H_2O:EtOH = 8:2 over time.

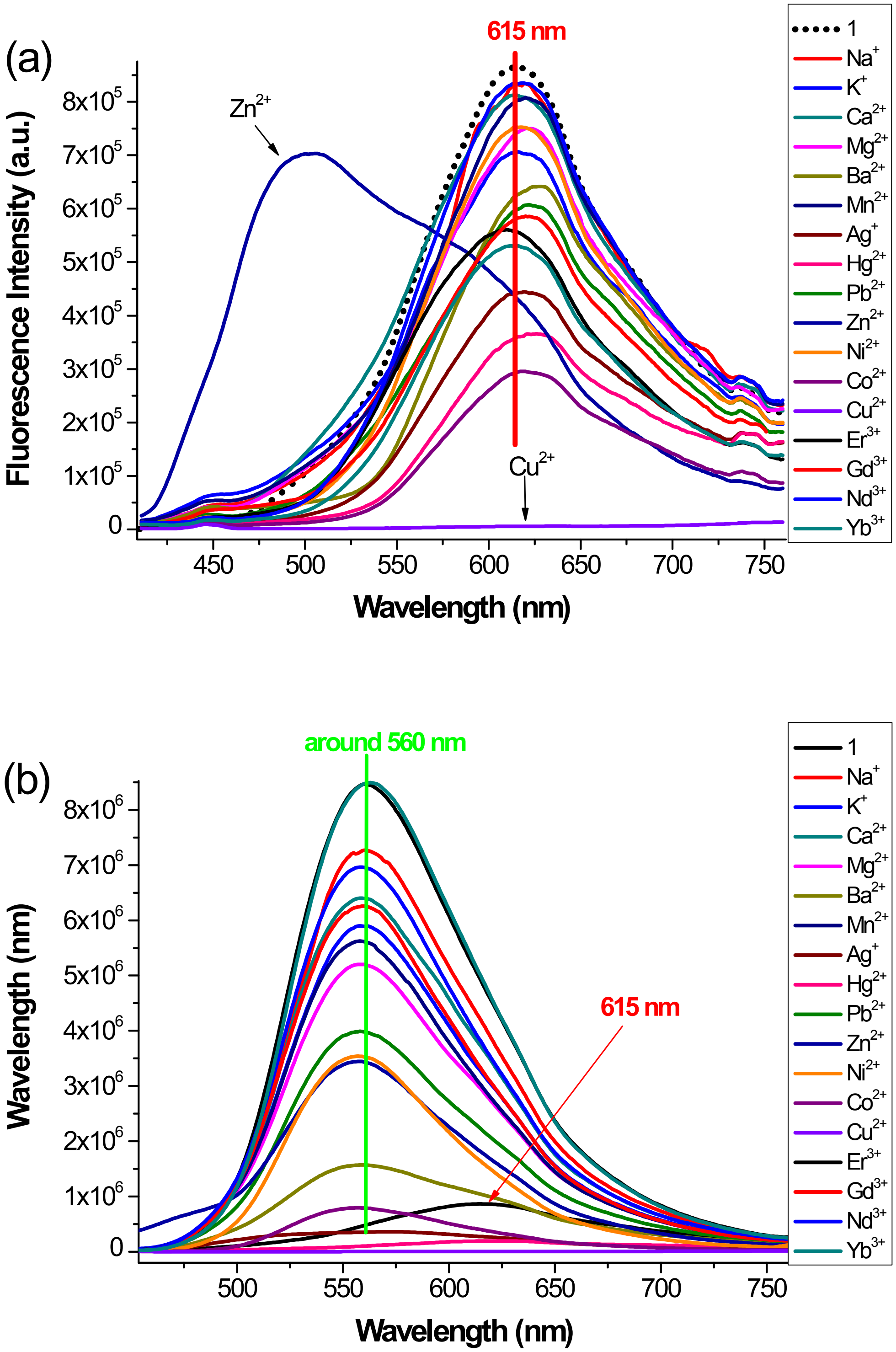

Fig. S6. Emission intensity of **1** (10 μM) at 615nm in H_2O:EtOH = 8:2 upon addition of 10.0 equiv of different metal ions excited at 390 nm (a), which was followed by addition of 10 equiv of Cr^{3+} (b).

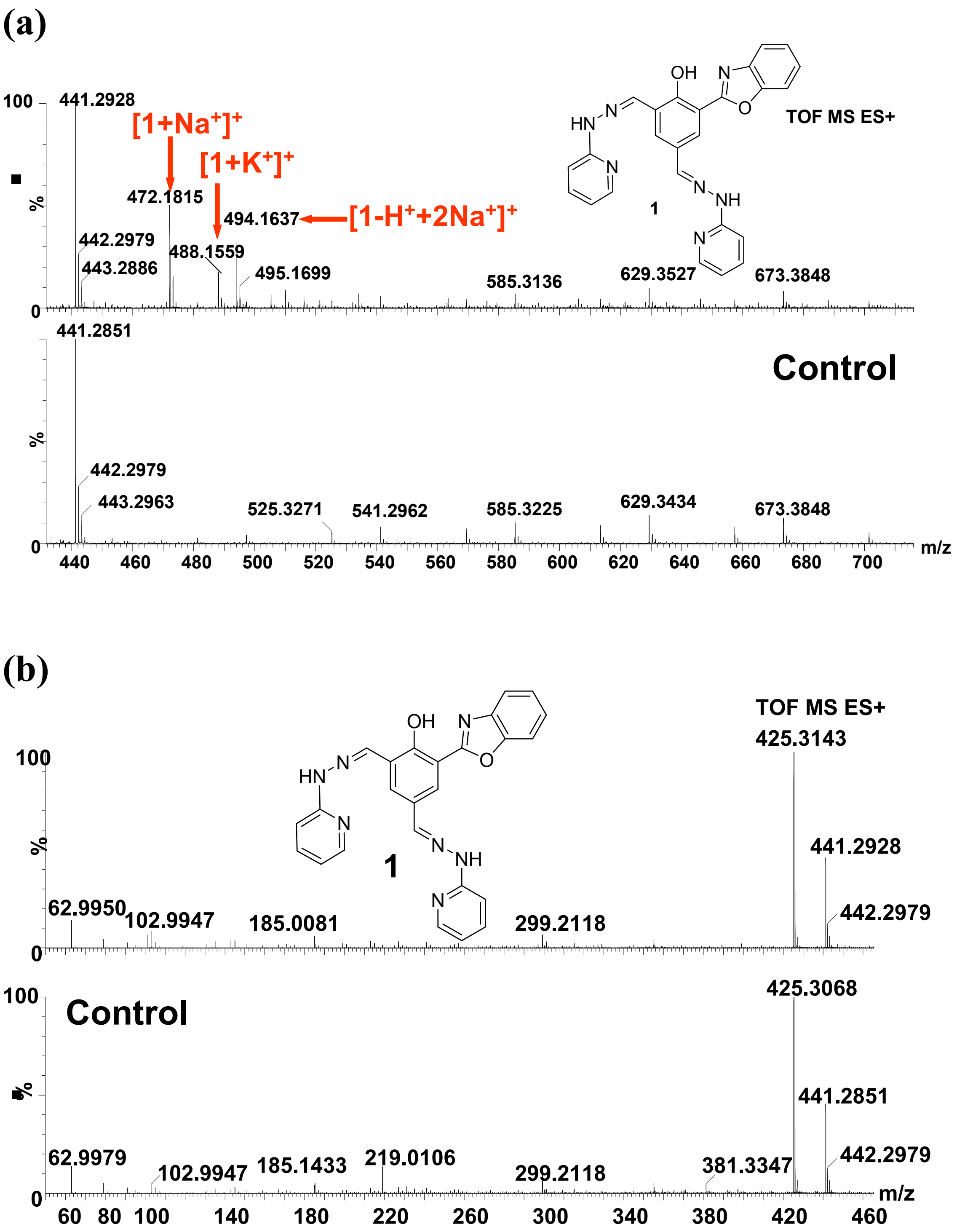

Fig. S7 TOF-MS-ES$^+$ of **1** (10 μM) in H_2O:EtOH = 8:2. (a) The control was obtained by only injecting the solvent (H_2O:EtOH = 8:2) without **1**. Calcd for $C_{25}H_{19}N_7O_2Na$, [**1**+Na$^+$]$^+$, 472.1498, found, 472.1815; calcd for $C_{25}H_{19}N_7O_2K$, [**1**+K$^+$]$^+$, 488.1237, found, 488.1559; calcd for $C_{25}H_{18}N_7O_2KNaNa$, [**1**-H$^+$+2Na$^+$]$^+$, 494.1317, found, 494.1637; (b) There are not clear decomposed species found in the range 50-470 (m/z), which tells **1** is quite stable in Mass mode.

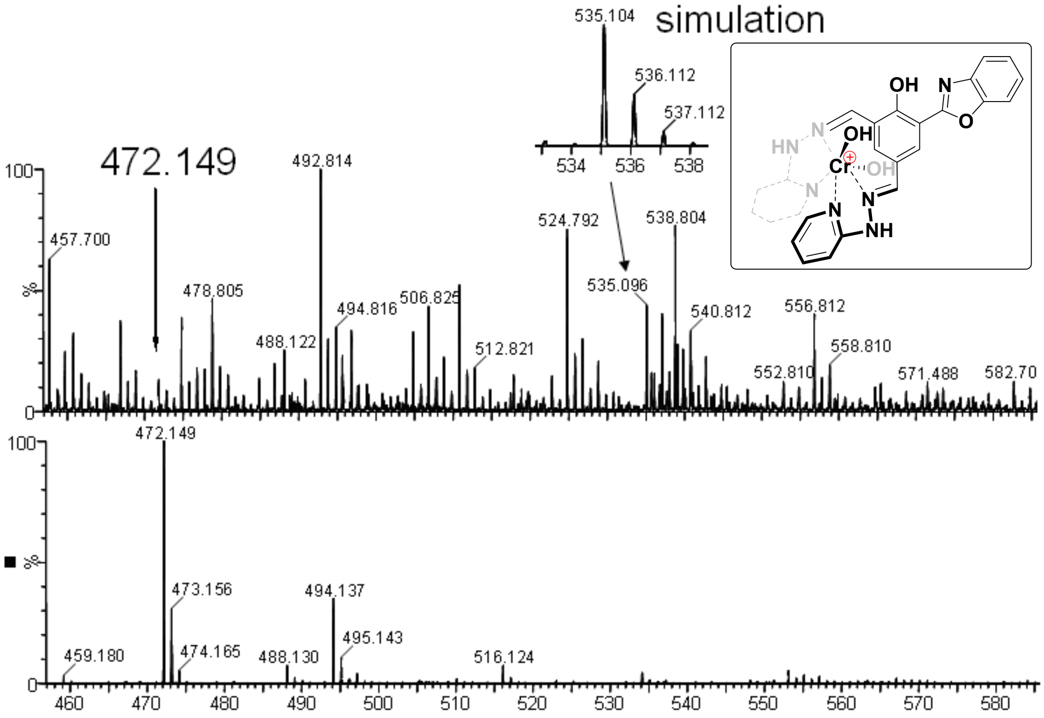

Fig. S8a. ESI-Mass of [**1+Cr^{3+}**] in aqueous (H_2O:EtOH = 8:2): calcd for $C_{25}H_{19}N_7O_2Na$, [M+Na$^+$]$^+$, 472.149, found, 472.149; calcd for $C_{25}H_{19}N_7O_2K$, [M+K$^+$]$^+$, 488.124, found, 488.130; calcd for $C_{25}H_{19}N_7O_2K$, [M-H$^+$+Na$^+$+Na$^+$]$^+$, 494.132, found, 494.137; calcd for $C_{25}H_{21}N_7O_4Cr$, [**1**+Cr^{3+}+2(OH)$^-$]$^+$ = 535.104, found 535.096.

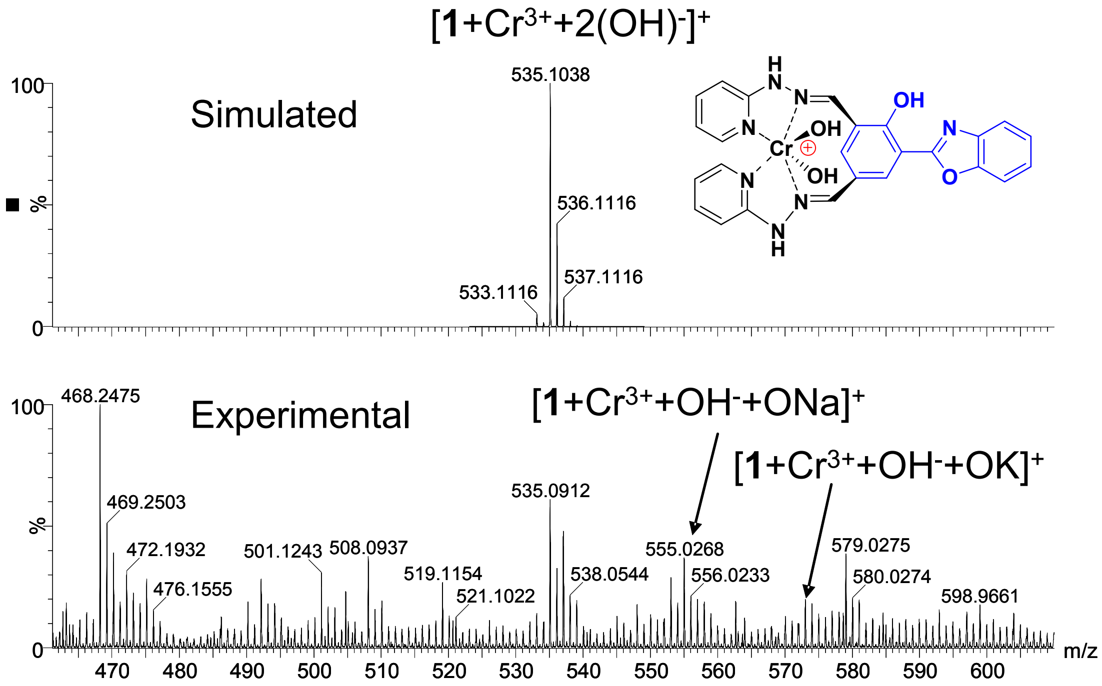

Fig. S8b. Repeated ESI-Mass for [**1+Cr^{3+}**] in aqueous (H_2O:EtOH = 8:2).

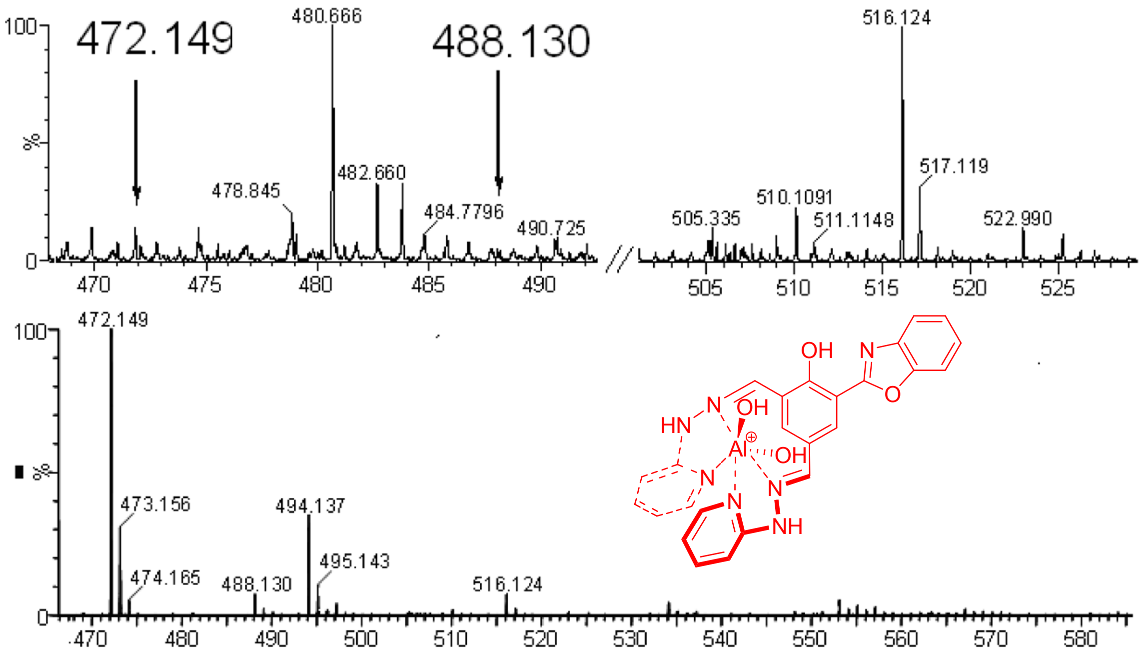

Fig. S8c. ESI-Mass of [**1**+Al^{3+}] in aqueous (H_2O:EtOH = 8:2): calcd for $C_{25}H_{21}N_7O_4Al$, [**1**+Al^{3+}+2$(OH)^-$]$^+$ = 510.1465, found 510.1091.

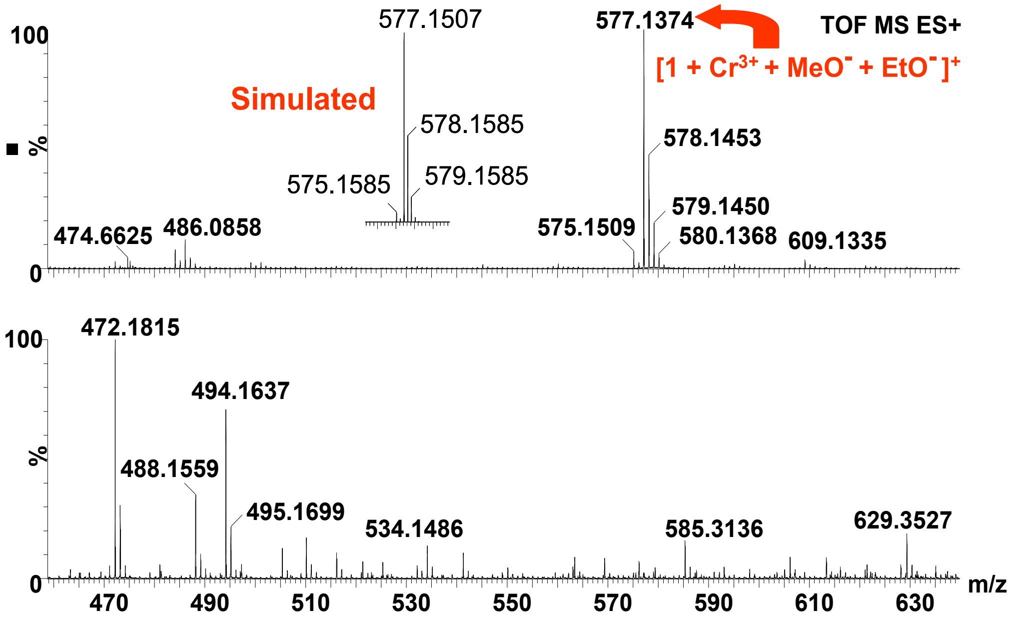

Figure 8d. Bottom panel: TOF-Mass-ES$^+$ spectra of dye **1** (peak $[1+Na^+]^+$ = 472.182, peak $[1+K^+]^+$ = 488.156, and $[1-H^+-2Na^+]^+$ = 494.164; Top panel: TOF-Mass-ES$^+$ spectra of its Cr^{3+} complex 2 obtained in EtOH:MeOH = 1:7.

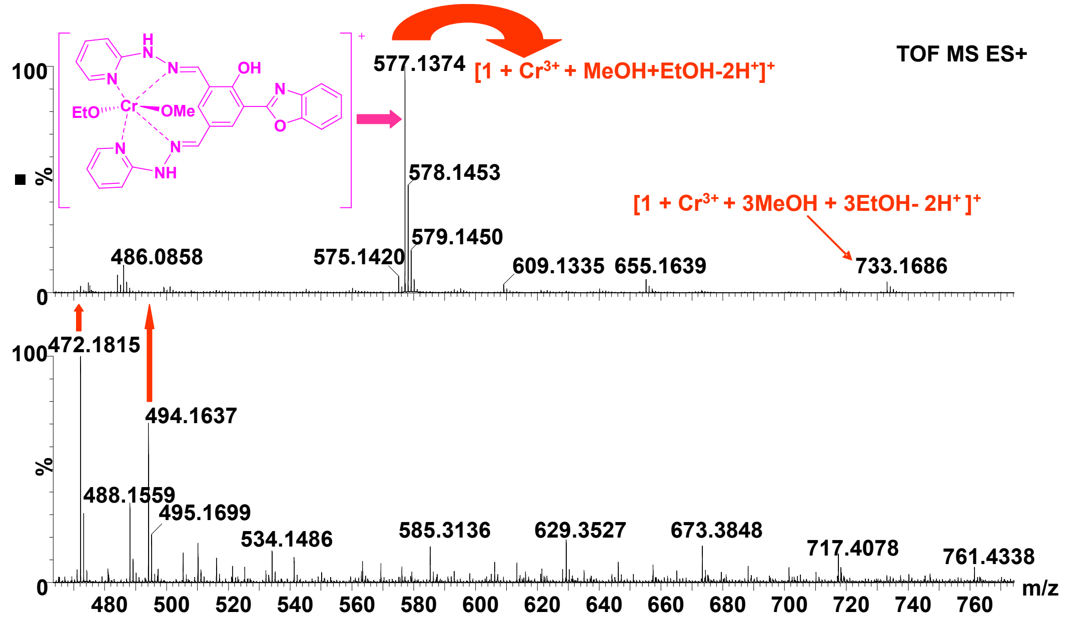

Fig 8e Bottom panel: TOF-Mass-ES$^+$ spectra of dye **1** (peak $[\mathbf{1}+\mathrm{Na}^+]^+$ = 472.182, peak $[\mathbf{1}+\mathrm{K}^+]^+$ = 488.156, and $[\mathbf{1}\text{-}\mathrm{H}^+\text{-}2\mathrm{Na}^+]^+$ = 494.164; Top panel: TOF-Mass-ES$^+$ spectra of its Cr^{3+} complex **2** obtained in EtOH:MeOH = 1:7 (In MS mode, potentials of **18V and 4V** were applied to the trap and collision cells respectively).

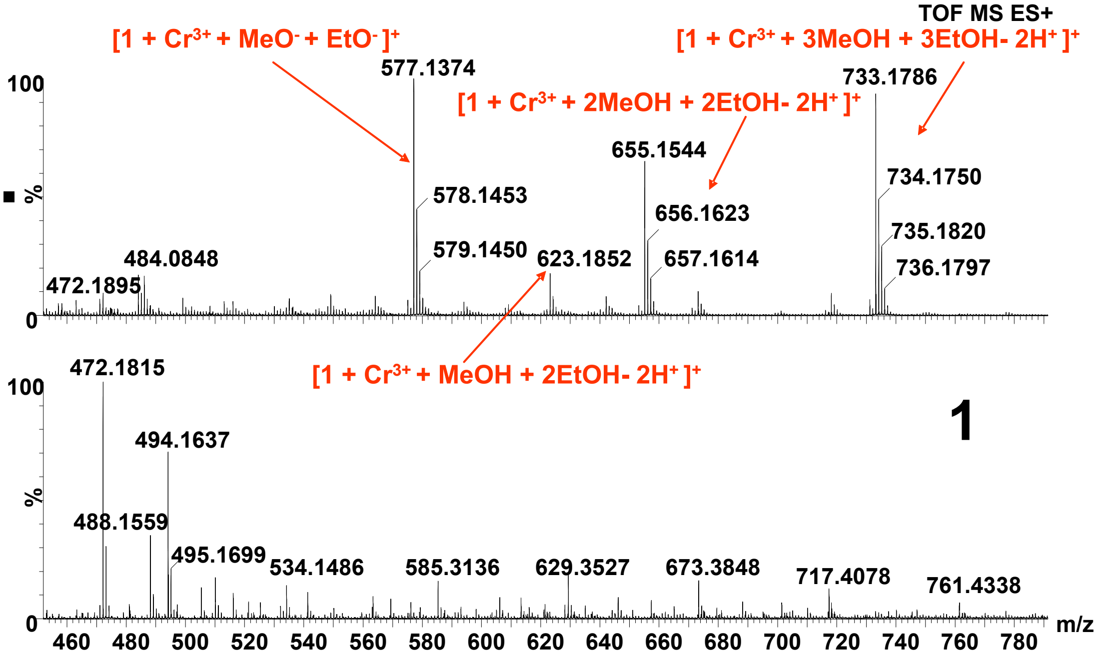

Fig S8f Bottom panel: TOF-Mass-ES$^+$ spectra of dye **1** (peak $[\mathbf{1}+\mathrm{Na}^+]^+$ = 472.182, peak $[\mathbf{1}+\mathrm{K}^+]^+$ = 488.156, and $[\mathbf{1}\text{-}\mathrm{H}^+\text{-}2\mathrm{Na}^+]^+$ = 494.164; Top panel: TOF-Mass-ES$^+$ spectra of its Cr^{3+} complex **2** obtained in EtOH:MeOH = 1:7 (In MS mode, potentials of **6V and 4V** were applied to the trap and collision cells respectively).

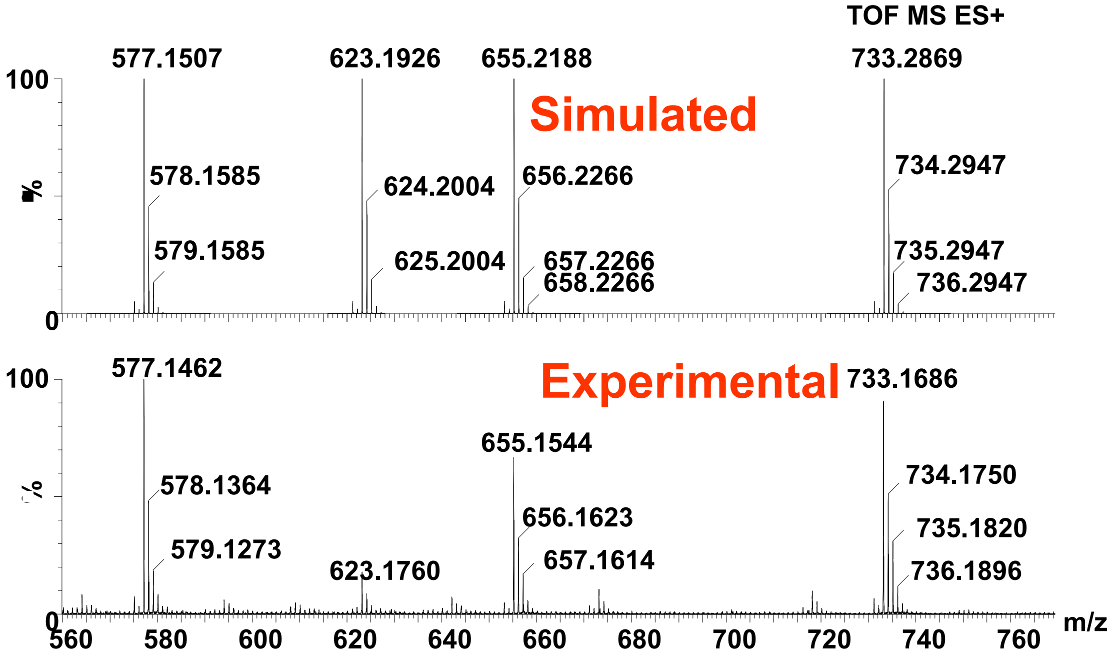

Fig S8g Bottom panel: TOF-Mass-ES$^+$ spectra of its Cr^{3+} complex **2** obtained in EtOH:MeOH = 1:7 (In MS mode, potentials of **6V and 4V** were applied to the trap and collision cells respectively) with corresponding simulation (top panel).

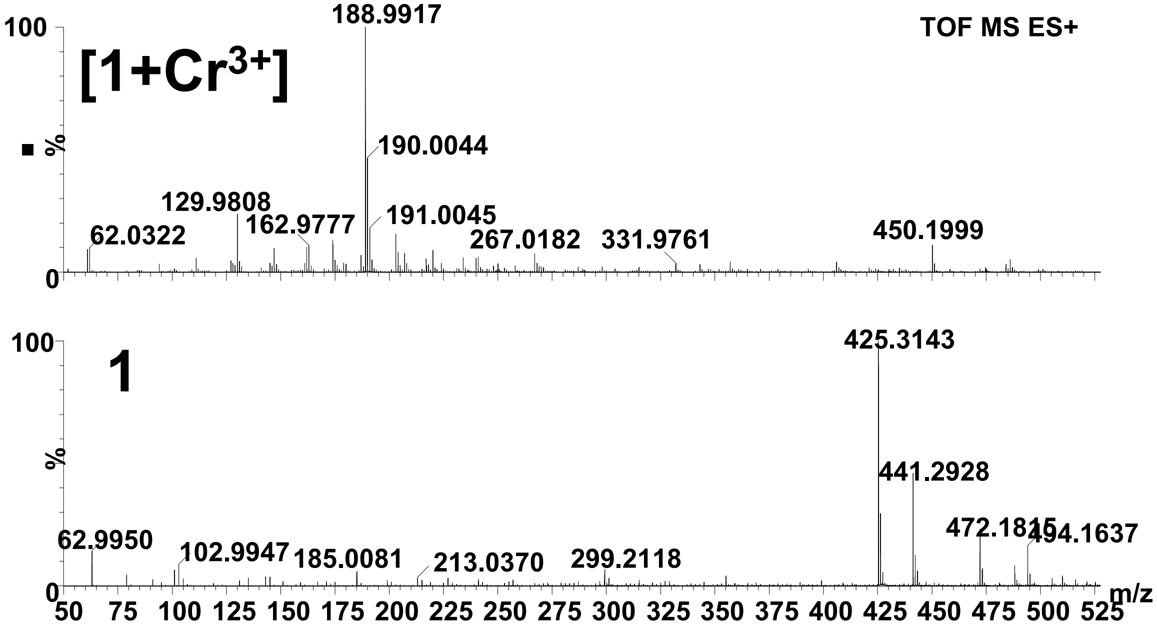

Fig S8h Bottom panel: TOF-Mass-ES$^+$ spectra of dye **1** (peak [**1**+Na$^+$]$^+$ = 472.182, peak [**1**+K$^+$]$^+$ =488.156, and [**1**-H$^+$-2Na$^+$]$^+$ = 494.164; Top panel: TOF-Mass-ES$^+$ spectra of its Cr^{3+} complex **2** (m/z from 50 to 527).

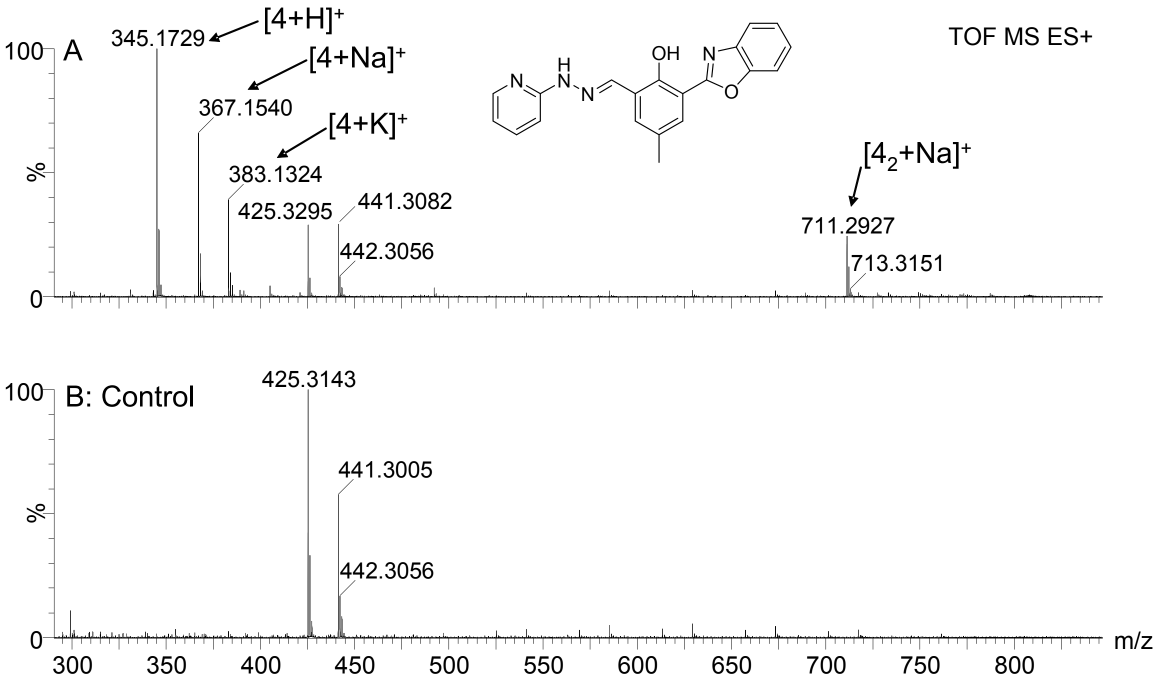

Fig S9a TOF-MS-ES$^+$ of **4:** Calcd for $C_{20}H_{17}N4O_2$, [**4**+H$^+$]$^+$, 345.1352, found, 345.1729; calcd for $C_{20}H_{16}N4O_2Na$, [**1**+Na$^+$]$^+$, 367.1171, found, 367.1540; calcd for $C_{20}H_{16}N4O_2K$, [**4**+K$^+$]$^+$, 383.0910, found, 383.1324; Bottom panel: The control was obtained by only injecting the solvent (H_2O:EtOH = 8:2) without **4.**

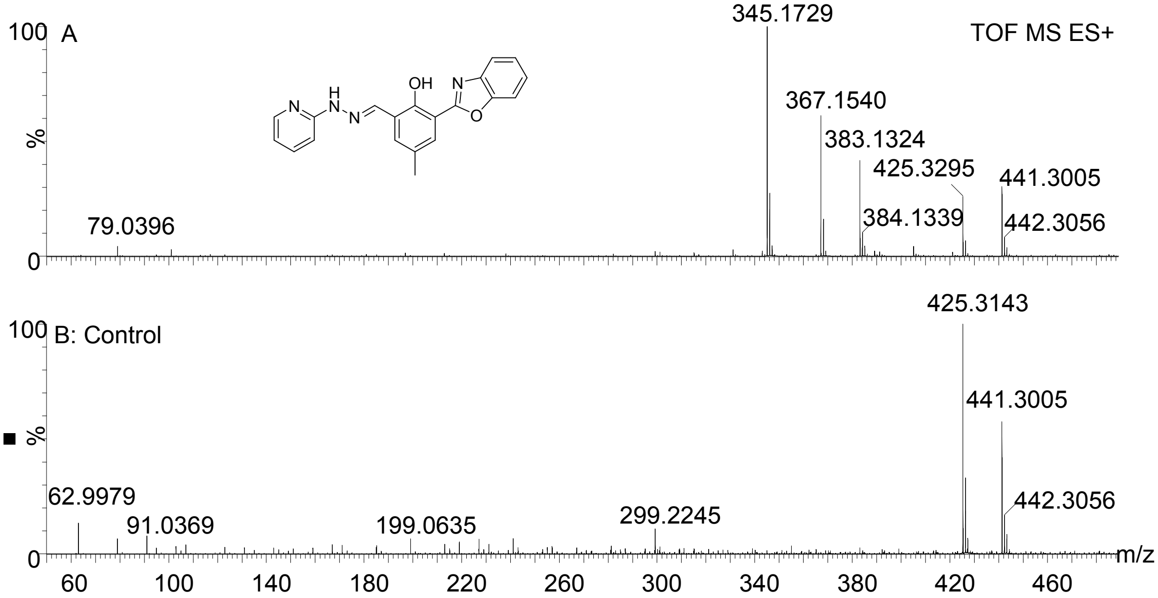

Fig S9b TOF-MS-ES$^+$ of **4:** Calcd for $C_{20}H_{17}N4O_2$, [**4**+H$^+$]$^+$, 345.1352, found, 345.1729; calcd for $C_{20}H_{16}N4O_2Na$, [**1**+Na$^+$]$^+$, 367.1171, found, 367.1540; calcd for $C_{20}H_{16}N4O_2K$, [**4**+K$^+$]$^+$, 383.0910, found, 383.1324; Bottom panel: The control was obtained by only injecting the solvent (H_2O:EtOH = 8:2) without **4.** There are not clear decomposed species found in the range 50-470 (m/z), which tells **4** is quite stable in Mass mode.

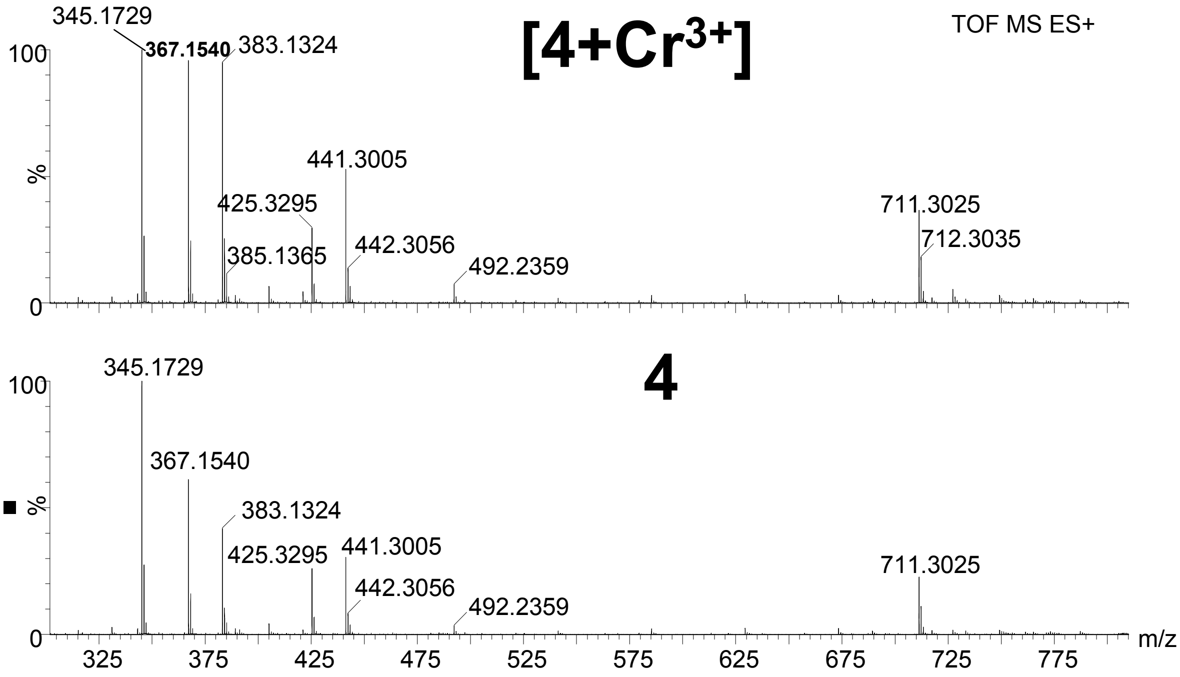

Fig. S9c TOF-MS-ES$^+$ of **4** and [**4**+Cr^{3+}]: no clear interaction between **4** and Cr^{3+} was observed by Mass, which is consistent with the UV-vis and Fluorescence data.

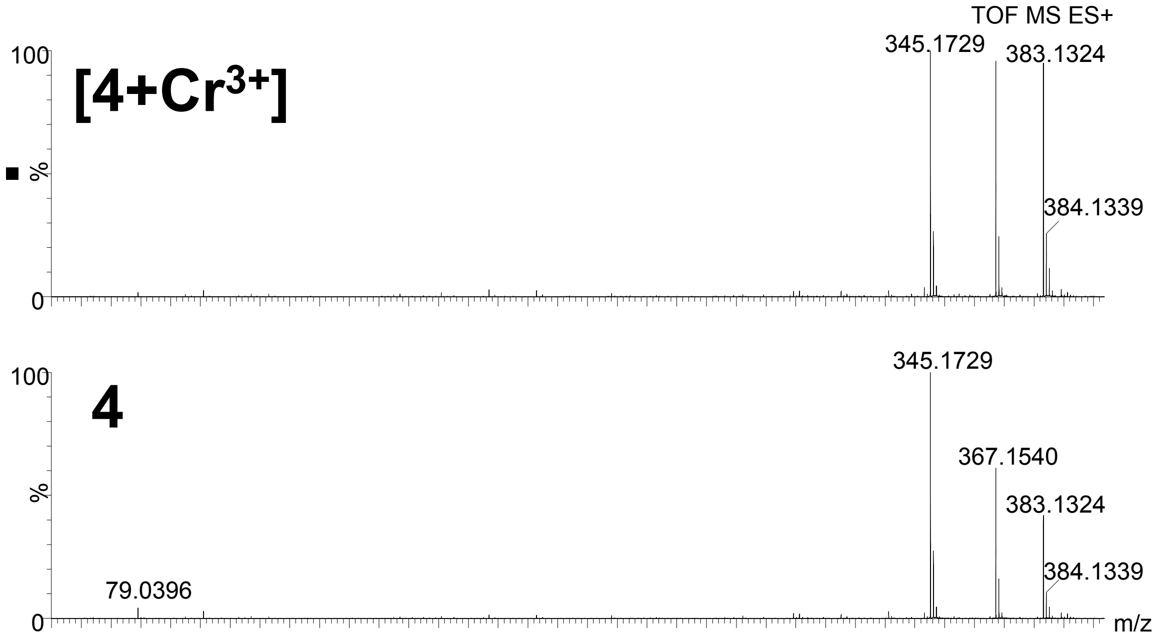

Fig. S9d TOF-MS-ES$^+$ of **4** and [**4**+Cr^{3+}]: no clear interaction between **4** and Cr^{3+} was observed by Mass, which is consistent with the UV-vis and Fluorescence data. There are not clear decomposed species found in the range 50-470 (m/z), which tells **4** and [**4**+Cr^{3+}] are quite stable in Mass mode.

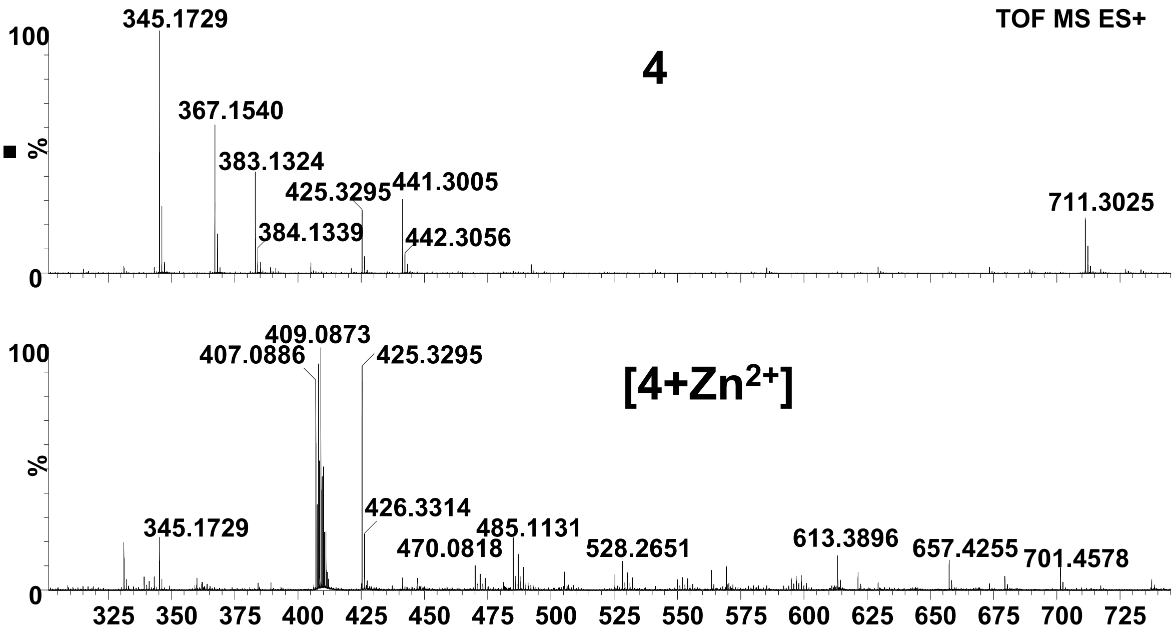

Fig. S9e TOF-MS-ES$^+$ of **4** (Top panel) and [**4**+Zn^{2+}] (bottom panel) in EtOH. One main species was found (See details in **Fig. S7f**).

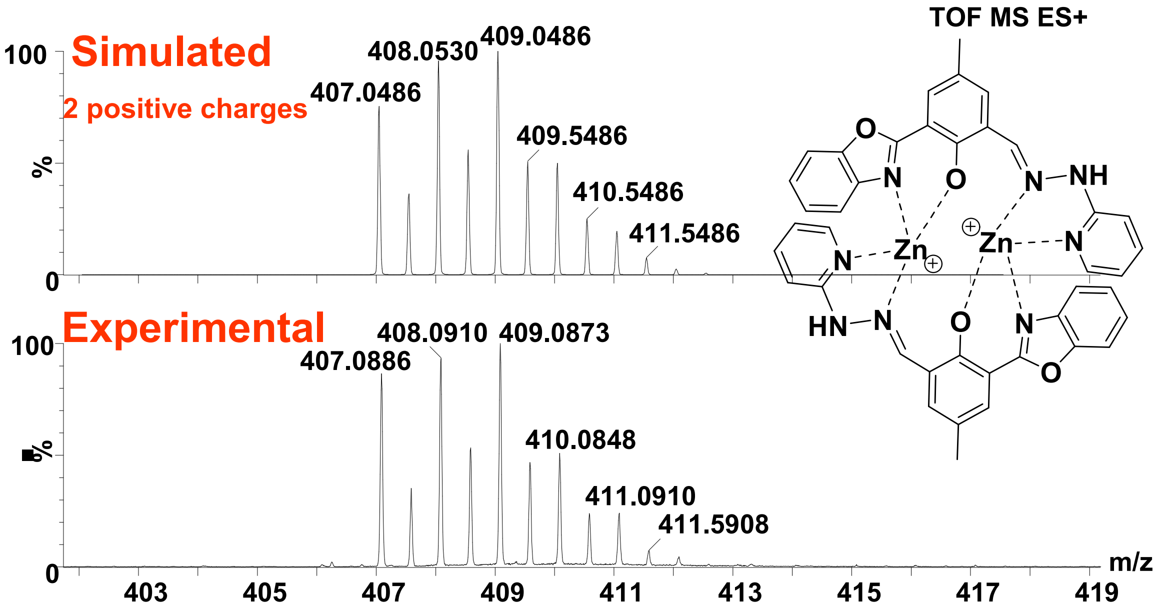

Fig. S9f TOF-MS-ES$^+$ of [**4**+Zn^{2+}] (bottom panel) with its simulation (Top panel): The complexes detected show 2 positive charges, which reveals a dimer structure.

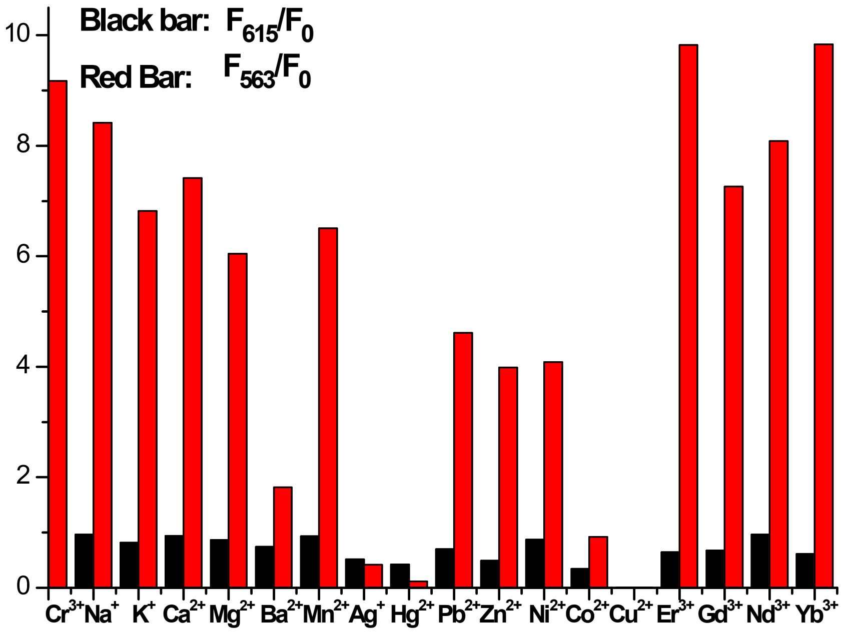

Fig S10a. Emission intensity of **1** (10 μM) at 615nm in H_2O:EtOH = 8:2 upon addition of 10.0 equiv of different metal ions excited at 390 nm (Black bars). Red bars represent the fluorescence intensity at 563 nm with subsequent addition of 10 equiv. of Cr^{3+}.

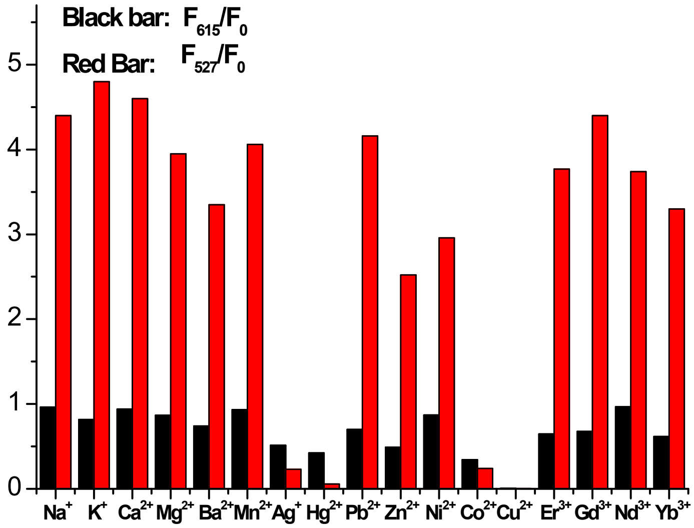

Fig S10b Emission intensity of **1** (10 μM) at 615nm upon addition of 10.0 equiv of different metal ions excited at 390nm (Black bars); F_0 is the fluorescence intensity of free ligand **1** (10 μM) at 615nm in H_2O:EtOH = 8:2. Red bars represent the fluorescence intensity with subsequent addition of 10 equiv. of Al^{3+} observed at 527 nm.

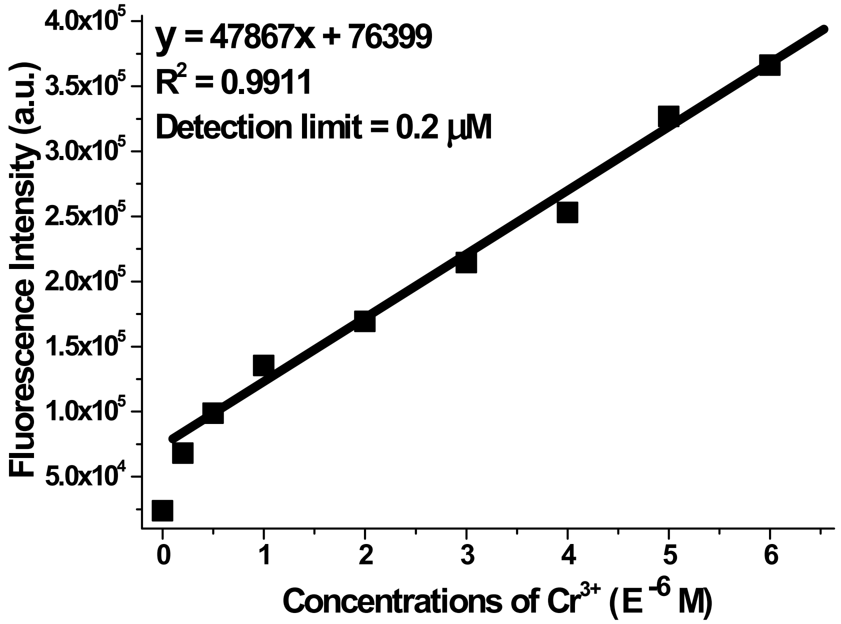

Fig. S11 Fluorescence intensity of **1**(1 μM) with different concentrations of Cr^{3+} in aqueous (H_2O:EtOH = 8:2), which showed linear range from 1-6 μM. The detection limit was calculated as 0.2μM for Cr^{3+}.

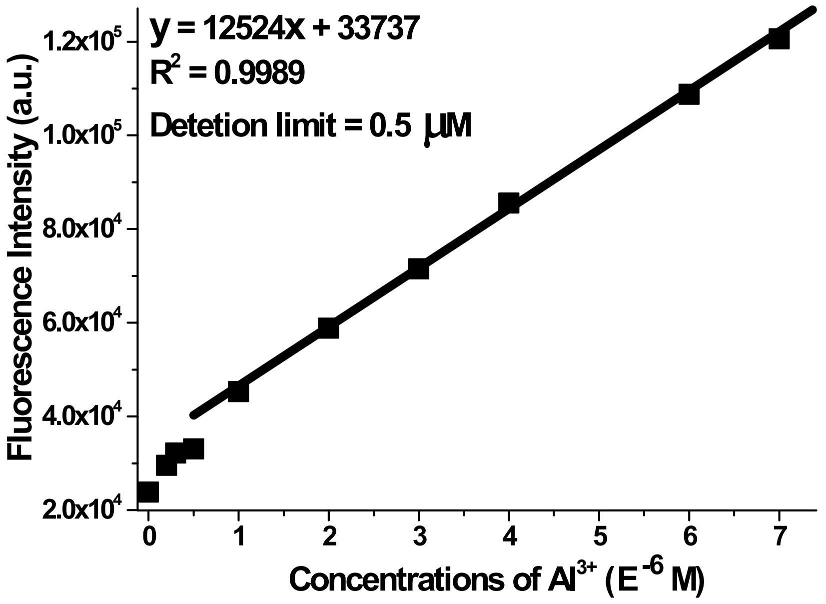

Fig. S12 Fluorescence intensity of **1**(1 μM) with different concentrations of Al^{3+} in aqueous (H_2O:EtOH = 8:2), which showed linear range from 1-6 μM. The detection limit was calculated as 0.5μM for Al^{3+}.

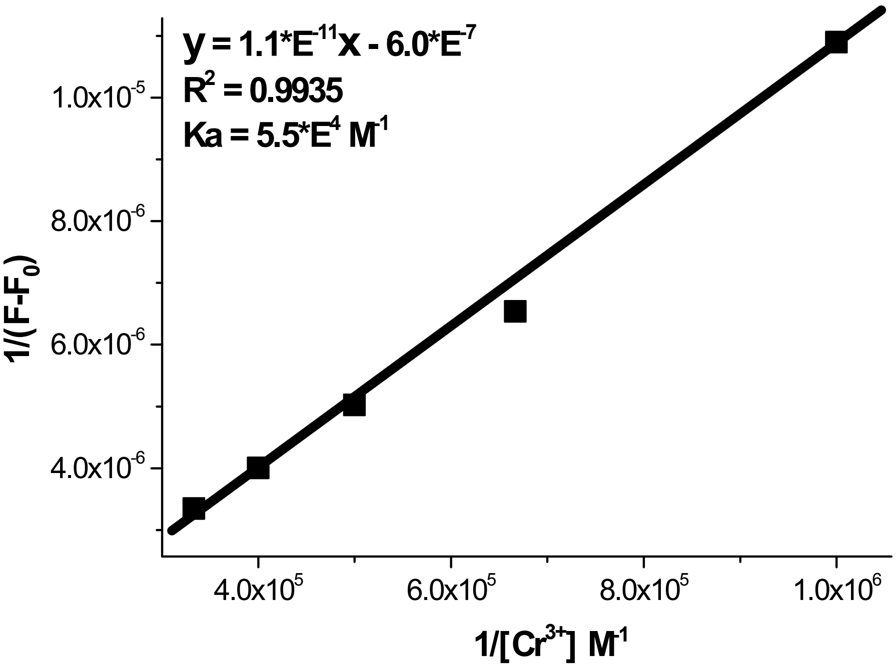

Fig. S13 Benesi–Hildebrand plot of **1** with **Cr^{3+}** in H_2O:EtOH = 8:2. The excitation wavelength was 360 nm and the observed wavelength was 560 nm. The binding constant was 5.5×10^4 M^{-1} for Cr^{3+} binding with **1**.

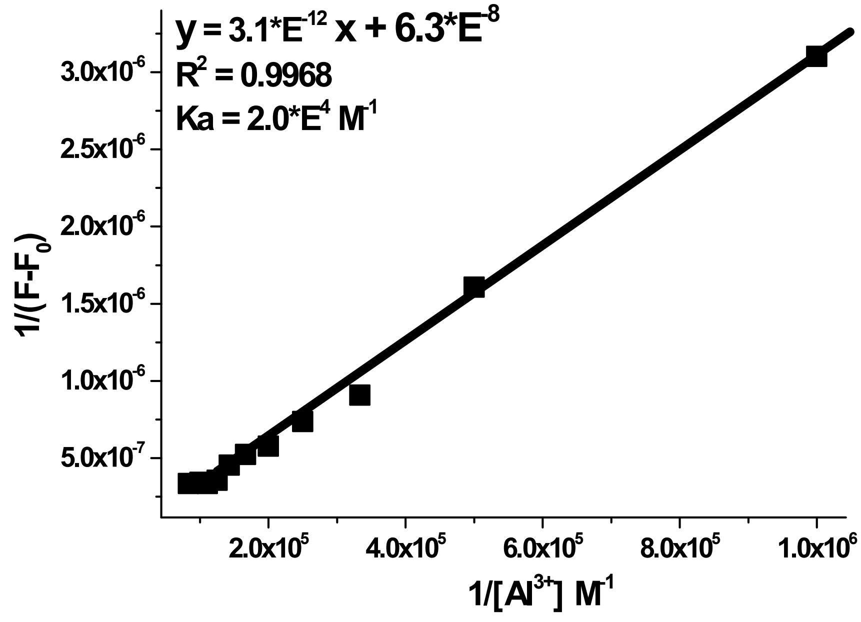

Fig. S14 Benesi–Hildebrand plot of **1** with **Al^{3+}** in H_2O:EtOH = 8:2. The excitation wavelength was 360 nm and the observed wavelength was 527 nm. The binding constant was 2.0×10^4 M^{-1} for Al^{3+} binding with **1**.

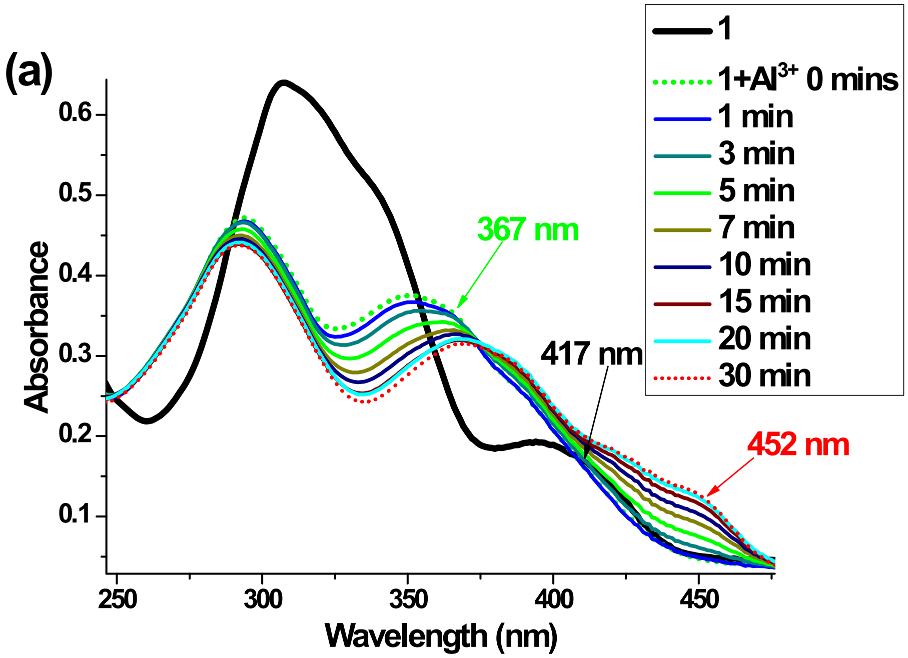

Fig. S15a UV-vis of **1** upon addition of 10 equiv. of Al^{3+} in EtOH changed with time.

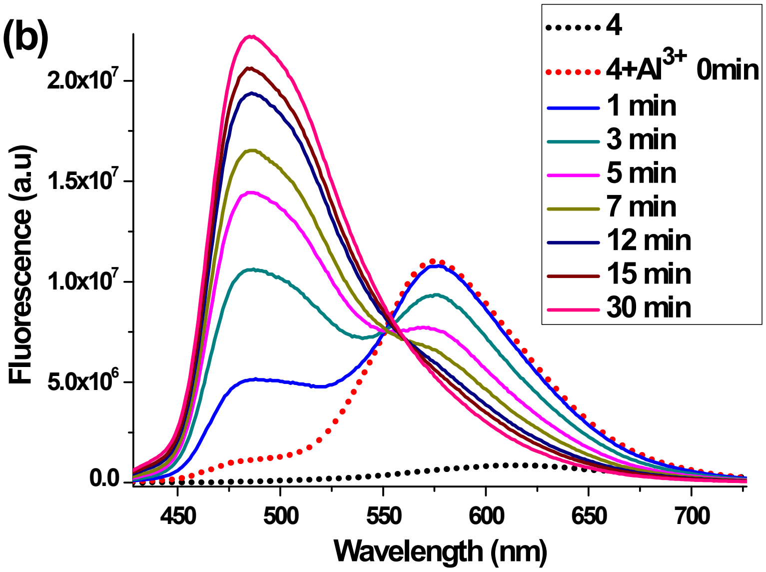

Fig. S15b Fluorescence of **1** upon addition of 10 equiv. of Al^{3+} in EtOH changed with time.

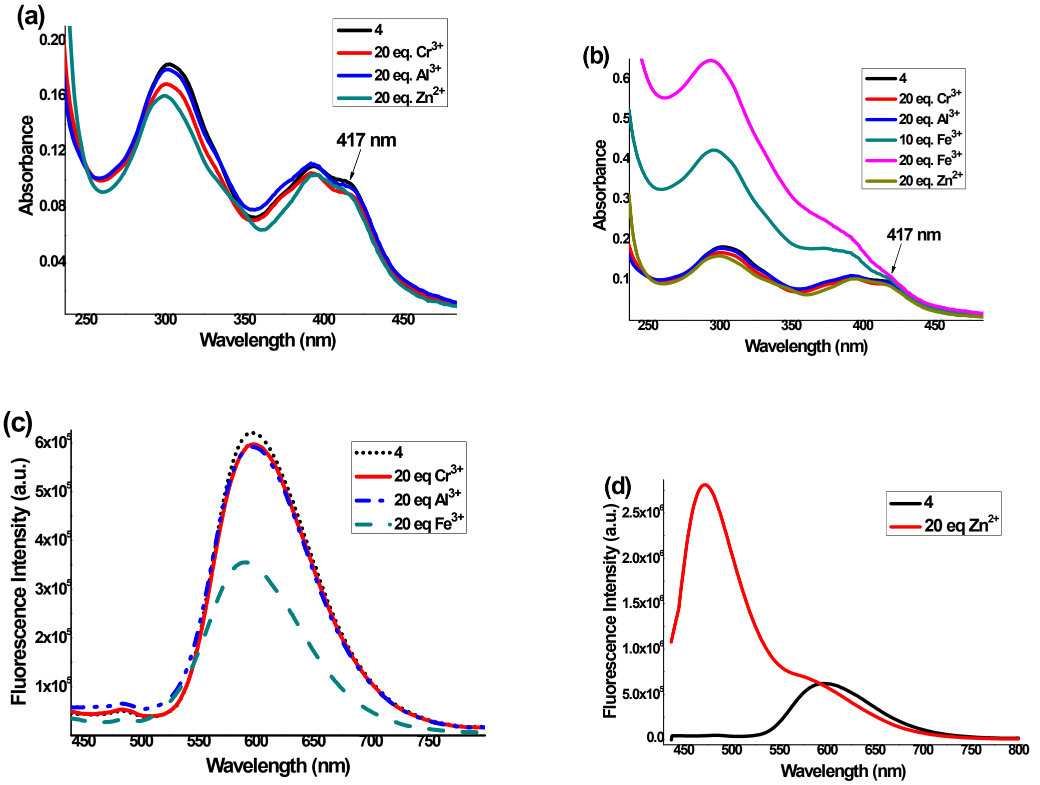

Figure S16 UV-vis (top) and fluorescence spectra (bottom) of **4** upon addition of 20 equiv. of metal ions in aqueous: (H_2O:EtOH = 8:2).

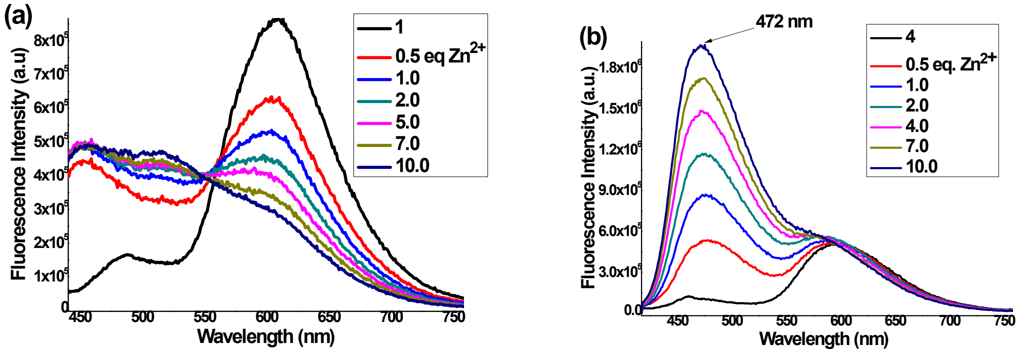

Figure S17 Fluorescence intensity of **1** (a) and **4** (b) upon addition of different equiv. of Zn^{2+} in aqueous (H_2O:EtOH = 8:2). **4** turned on the fluorescence with blue shift due to the enabled ESIPT, while **1** greatly quenched the fluorescence probably due the existing imine (-N=CH-) functional group.

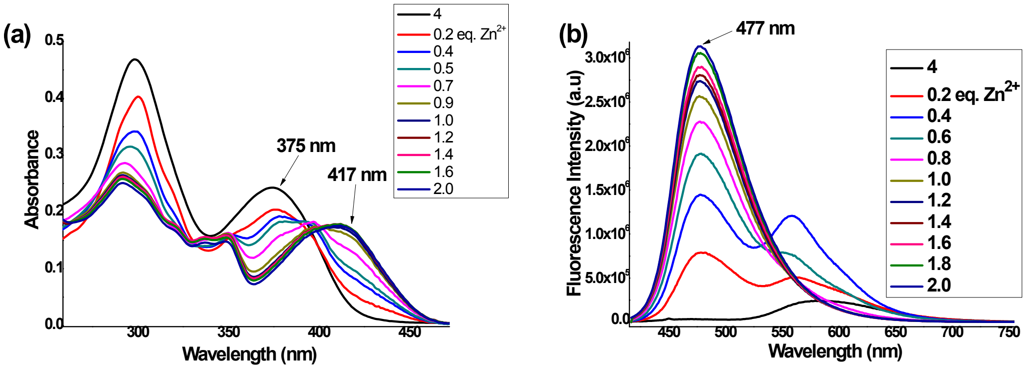

Figure S18 UV-vis (a) and fluorescence (b) titration of **4** upon addition of different equiv. of Zn^{2+} in EtOH.

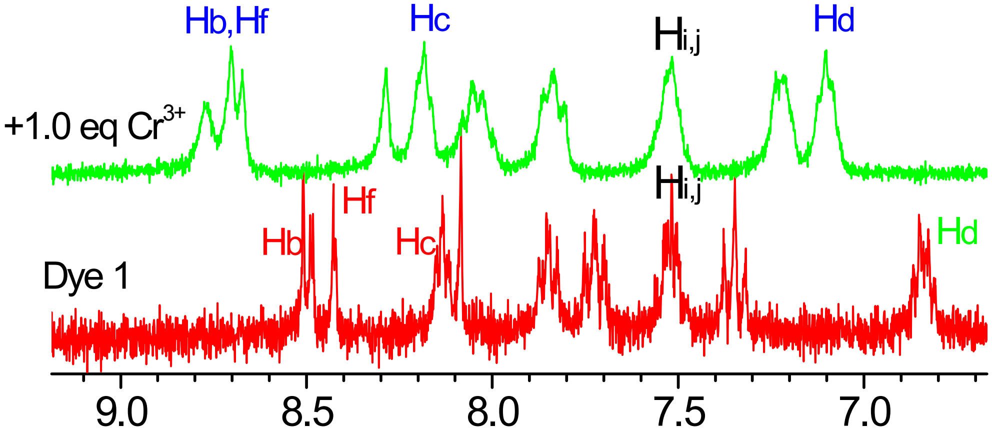

Figure S19 ^1H NMR of **1** upon addition of 1.0 equiv. of Cr^{3+} in CD_3OD:DMSO-d_6 (7:1).

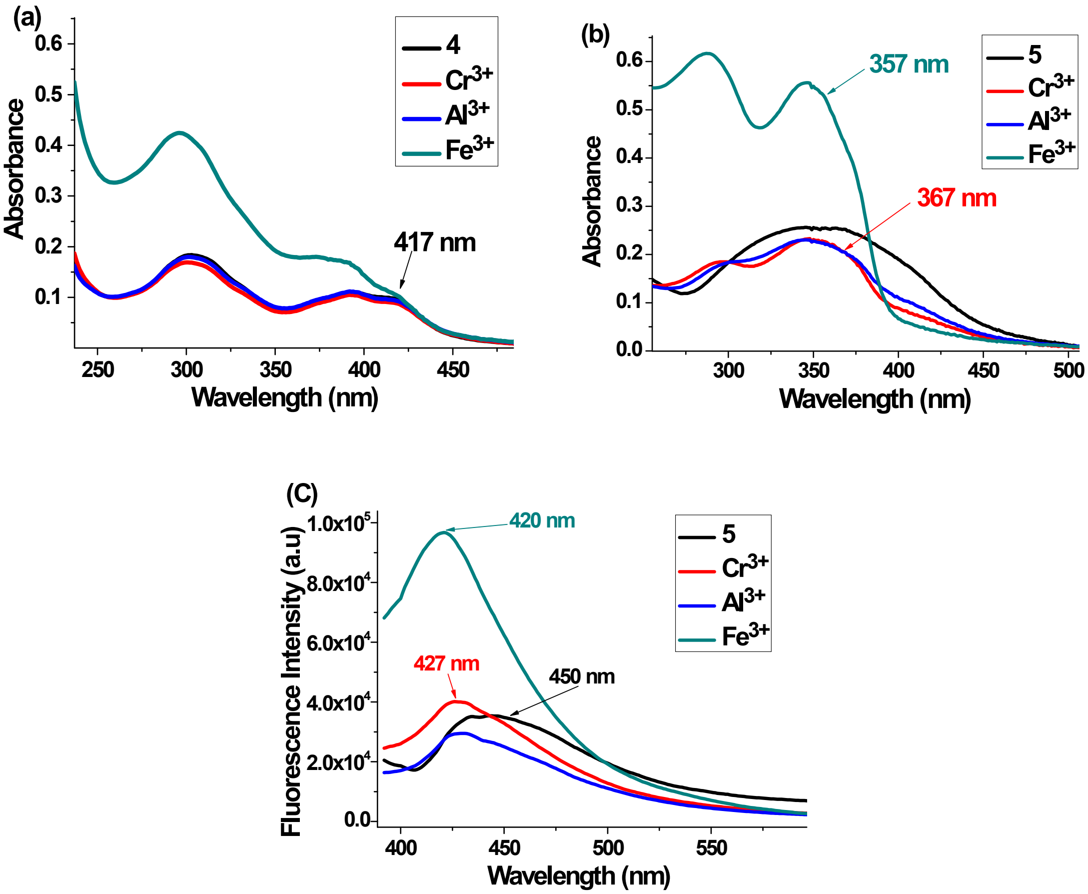

Figure S20 UV-vis (a) response of **4** upon addition of 10 equiv. of different metal ions in aqueous (8:2 = water : EtOH); UV-vis (b) and fluorescence (c) response of **5** upon addition of 10 equiv. of different metal ions in aqueous (8:2 = water : EtOH).

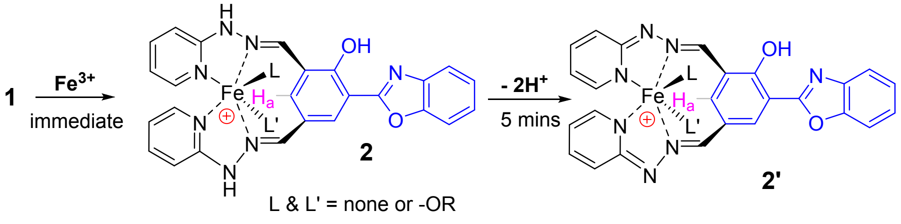

Scheme S1. Dye **1** and its Fe^{3+} complexes **2** and **2'**

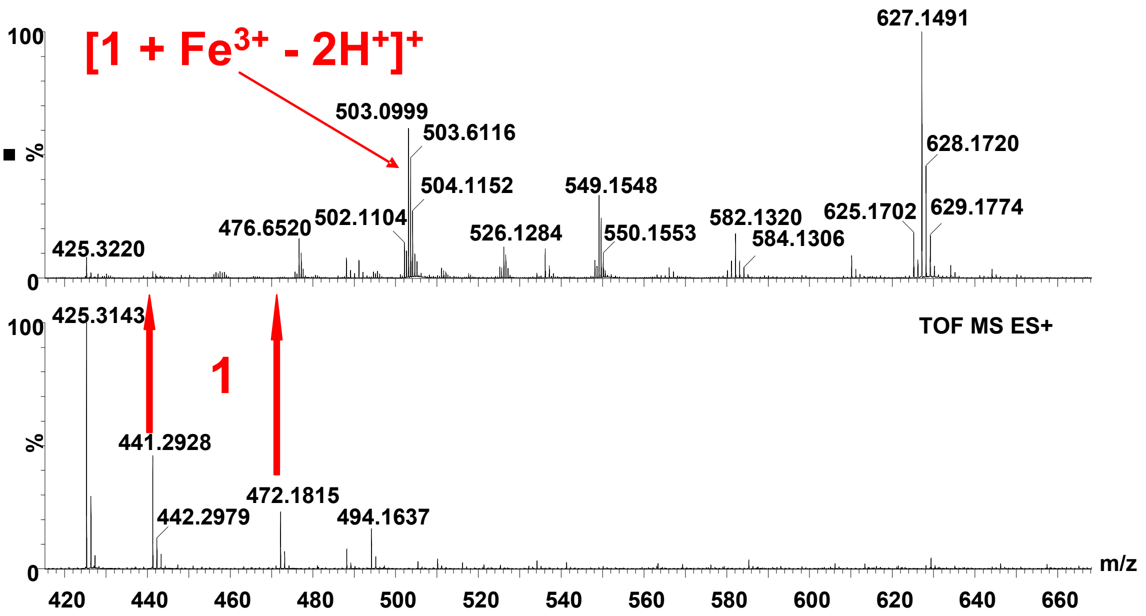

Figure S21a. Bottom panel: TOF-Mass-ES$^+$ spectra of dye **1** (peak $[1+Na^+]^+$ = 472.182, peak $[1+K^+]^+$ = 488.156, and $[1-H^+-2Na^+]^+$ = 494.164; Top panel: TOF-Mass-ES$^+$ spectra of its Fe^{3+} complex 2' obtained in EtOH:MeOH = 1:7.

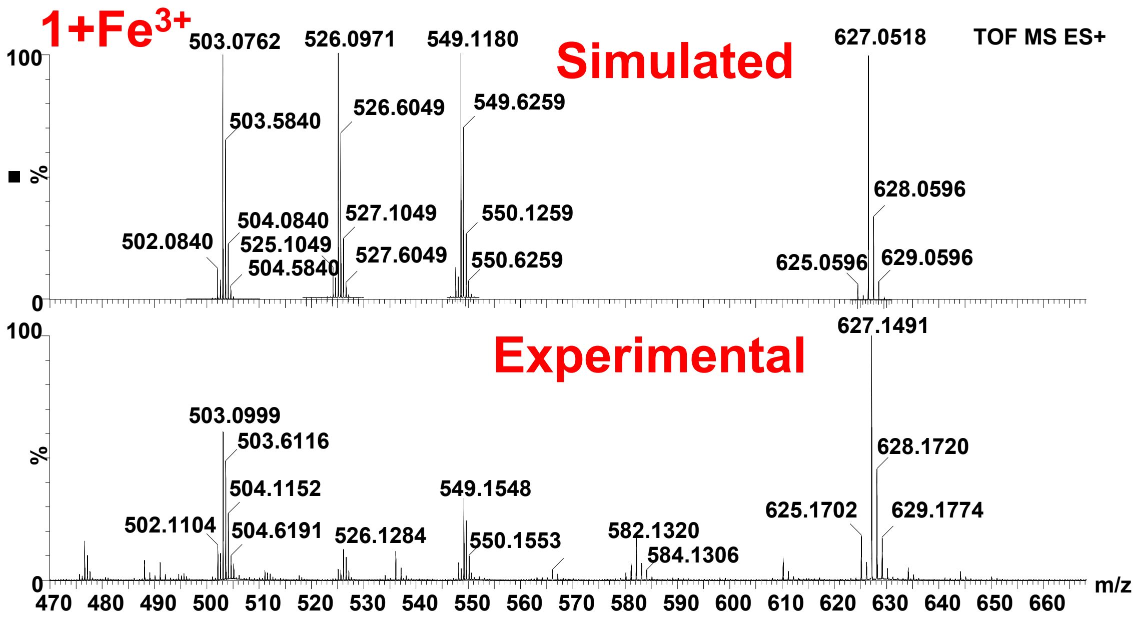

Fig S21b Bottom panel: TOF-Mass-ES$^+$ spectra of its Fe^{3+} complex **2'** obtained in EtOH:MeOH = 1:7 (In MS mode, potentials of **6V and 4V** were applied to the trap and collision cells respectively) with corresponding simulation (top panel).

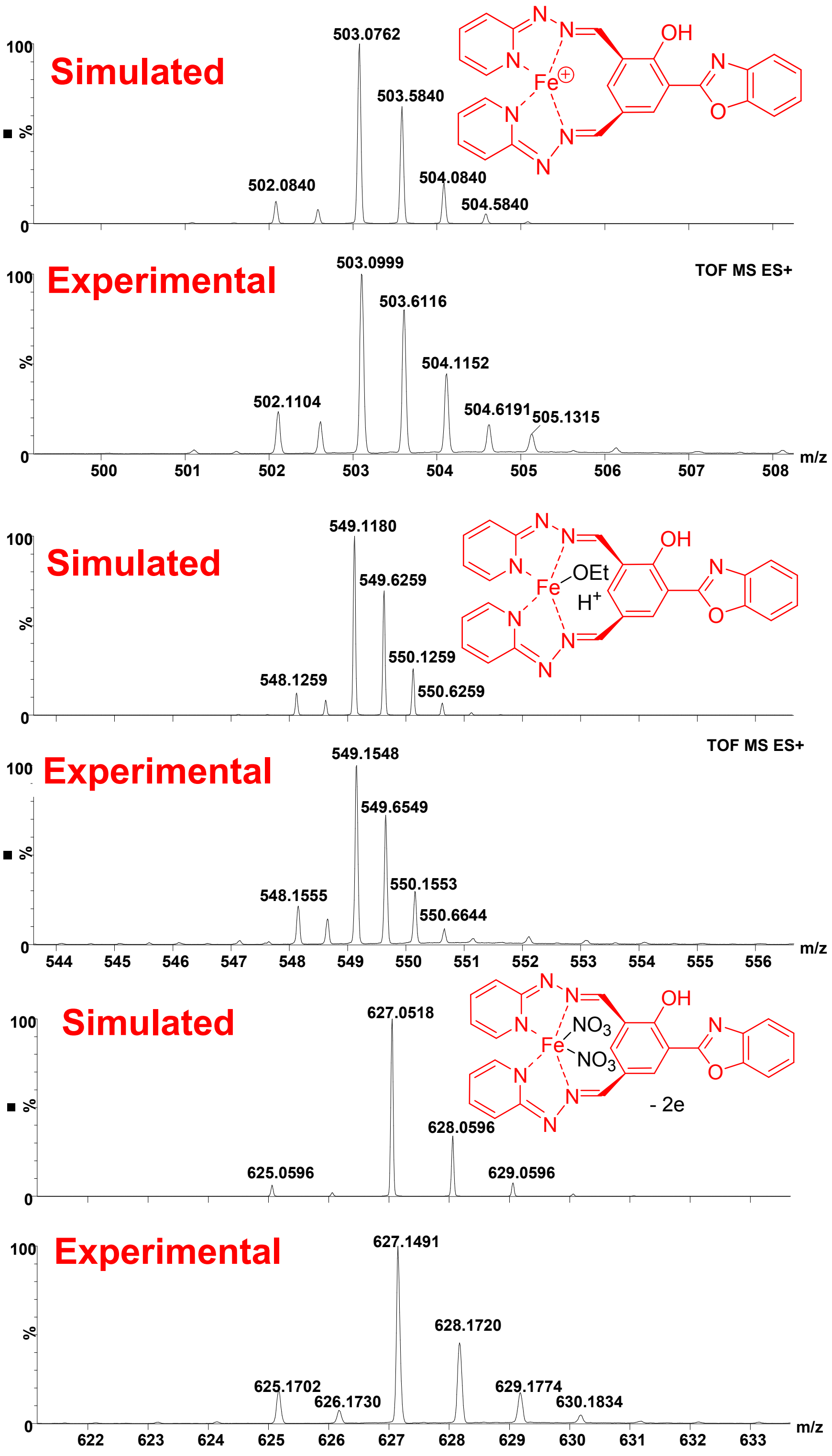

Fig S21c TOF-Mass-ES$^+$ spectra of the Fe^{3+} complexes **2’** obtained in EtOH:MeOH = 1:7 (In MS mode, potentials of **6V and 4V** were applied to the trap and collision cells respectively) with corresponding simulation.

^{1}H NMR of A:

^{1}H NMR of 1

^{13}C NMR of 1:

^{1}H NMR of 4

^{13}C NMR of 4

^{1}H NMR of D

^{13}C NMR of D

^{1}H NMR of 5

^{13}C NMR of 5